

NATIONAL ADVISORY COMMITTEE FOR AERONAUTICS

# WARTIME REPORT

ORIGINALLY ISSUED

February 1944 as  
Advance Restricted Report 4B02

FLIGHT TESTS OF THE THERMAL ICE-PREVENTION  
EQUIPMENT ON THE B-17F AIRPLANE

By Bonne C. Look

Ames Aeronautical Laboratory  
Moffett Field, California

**FILE COPY**

To be returned to  
the files of the National  
Advisory Committee  
for Aeronautics  
Washington, D. C.

276



WASHINGTON

NACA WARTIME REPORTS are reprints of papers originally issued to provide rapid distribution of advance research results to an authorized group requiring them for the war effort. They were previously held under a security status but are now unclassified. Some of these reports were not technically edited. All have been reproduced without change in order to expedite general distribution.

NATIONAL ADVISORY COMMITTEE FOR AERONAUTICS

ADVANCE RESTRICTED REPORT

FLIGHT TESTS OF THE THERMAL ICE-PREVENTION  
EQUIPMENT ON THE B-17F AIRPLANE

By Bonne C. Look

SUMMARY

Performance tests of the thermal ice-prevention equipment, developed for the B-17F airplane by the Ames Aeronautical Laboratory, have been conducted at the NACA Ice Research Project, Minneapolis, Minn., in cooperation with the Materiel Command, U.S. Army Air Forces. Temperatures of the heated surfaces, structure, and circulating air and the air-flow rate and quantity of heat through the system were obtained during flights in dry air (no visible moisture) and in natural icing conditions. Observational and photographic data were obtained of the susceptibility of the protected and unprotected areas of the airplane to ice formations.

The performance tests of the thermal ice-prevention equipment indicated that, with a few exceptions, satisfactory protection was provided for all protected surfaces. The heat supplied to the empennage was not sufficient to provide complete protection in the most severe icing conditions encountered, and the wing tips were subject to icing. For all parts of the airplane where the design specifications were realized, protection was provided by the thermal ice-prevention equipment without apparent deleterious thermal effects on the structure. Where the specifications were not satisfied, the system failed to prevent completely the formation of ice. It was further substantiated by the results of the reported tests that sufficient data are available for the design of thermal ice-prevention equipment for airplanes which will provide protection from icing.

INTRODUCTION

For the past several years the NACA has been extensively engaged in an investigation of the prevention of

ice formation on airplanes by the use of thermal ice-prevention equipment utilizing the heat of the exhaust gases from the airplane's engines. As a part of this program, the AAL has designed and tested thermal ice-prevention equipment on a Lockheed 12A airplane (reference 1) and on a Consolidated B-24D airplane (reference 2). Also, at the request of the Materiel Command, U.S. Army Air Forces, the AAL has developed a thermal ice-prevention system for the Boeing B-17F airplane. A description of this design, an outline of the design analysis, and a presentation and discussion of flight-test thermal data secured in dry air are reported in reference 3.

The flight tests of the thermal ice-prevention equipment on the B-17F airplane reported herein have been conducted in natural icing conditions for the purpose of supplementing the flight tests described in reference 3, to study the operation of the ice-prevention system in icing conditions and to obtain thermal data which may assist in extending the development and use of this type of equipment. The flight operations were conducted at the NACA Ice Research Project, Minneapolis, Minn., during the months of January, February, and March, 1943. Flights were planned with the cooperation of the U.S. Weather Bureau and the Northwest Airlines dispatch office.

#### DESCRIPTION OF THE ICE-PREVENTION EQUIPMENT

The B-17F airplane equipped with the thermal ice-prevention system is illustrated in figure 1. Figure 2 is the general layout of the installation which is described in detail in reference 3. The details of the ice-prevention system design for the wing and empennage are shown in figures 3 to 7. The instrumentation of the equipment was the same as reported in reference 3; however, the exhaust-gas temperatures were not obtained for the tests conducted at the Ice Research Project. The thermocouple and venturi-meter locations are shown in figure 8. All temperatures were determined with iron-constantan thermocouples and a Lewis direct-reading potentiometer.

Facilities for heating the pilot's and copilot's windshields were not included in the ice-prevention equipment installed at the AAL because an extensive investigation was being conducted elsewhere by the Army Air

Forces. The need of a windshield heating system became apparent, however, after the initial flights in icing conditions had been made. Hence, a temporary heating system for the pilot's windshield was installed which utilized the service windshield and defrosting installation. The service windshield consisted of two panes of glass with an approximate  $3/8$ -inch gap between, maintained by a plastic spacer around the edges of the glass. The defroster located at the forward lower corner of the windshield directed heated air, supplied by the service cabin-heating system, against the inner surface of the inner pane of glass. Slots were cut in the forward and aft plastic spacers of the windshield and the defroster outlet was replaced with a distribution header to direct the heated air into the forward slot. The normal flow of heated air to the defroster was increased by the installation of a small blower, driven by a 1-horsepower electric motor, in the supply duct. The air passed between the two panes of glass and exhausted into the pilot's compartment through the slot in the aft edge of the windshield. Two thermocouples were installed in the system; one in the heated-air supply duct at the inlet side of the blower and one in the windshield air-exit gap. A method of obtaining the heated-air flow rate was not available.

A strut to serve as an unprotected surface for the observation of ice accumulations by the flight personnel was mounted on the left side of the fuselage at the aft edge of the radio compartment window. The use of an ice indicator which would automatically control the ice-prevention system had been considered, but was not employed on the test airplane.

The liaison radio service antenna lead-in wire, which extended from the upper surface of the left wing to the left side of the fuselage in a direction approximately  $45^\circ$  to the air stream, was replaced with a rubber-covered  $1/16$ -inch steel cable to decrease the effect of precipitation static on radio communication and withstand the loads imposed by heavy formations of ice.

#### TESTS

In general, the procedure followed during the icing flights was to make first a preliminary vertical and

horizontal traverse of the region of probable icing to establish the boundaries of the icing area, and to determine the severity of the icing condition. After the preliminary survey was completed, the airplane was flown in the icing region for a sufficient length of time to allow complete observations to be made of the operation of the thermal ice-prevention equipment. A total of seven flights in icing conditions and two in dry air was conducted. During four of the flights in icing conditions and the two in dry air, temperatures of the heated surfaces, structure, and circulating air were obtained. The air-flow rate and quantity of heat through the system were also determined. Observational and photographic data of the protection afforded by the thermal ice-prevention system were obtained during all the icing flights.

During the majority of the flights in icing regions the engines were operated at cruising-power conditions of approximately 28 inches of mercury manifold pressure and 1800 rpm engine speed. To investigate the effect of an increase in engine power on the operation of the ice-prevention equipment, one test was made at engine power conditions of approximately 31 inches of mercury manifold pressure and 2100 rpm engine speed.

The airplane was inspected after each flight in order to note ice accumulations on airplane parts not visible to the observers during flight and to study the formation of ice still adhering to the airplane.

## RESULTS

The conditions under which the tests were conducted are shown in table I. Variations in the rate of icing on different parts of the airplane made it impossible to define accurately the severity of the icing for the various conditions. A designation of the severity of the icing conditions, arbitrarily chosen to provide a means for comparing flights, has been included in table I. The lightest icing condition encountered has been designated as 1 and the most severe condition as 4. Flight, engine, and thermal data, which were taken for seven test conditions, are presented in tables II, III, and IV. Complete thermal data were not obtained during test 1; however, the data obtained have been included because the lowest temperature icing was encountered on this flight,

and a comparison of these data with the data taken during other flights is believed to be of interest. The thermal data include the quantity of heat supplied by the exchangers and the temperatures of the circulating air, heated surfaces, and structure. The chordwise distribution of the wing outer-panel skin temperature rise is presented in figures 9 to 15 for the seven tests. The thermocouple designations given in the tables correspond to those shown in figure 8. In the interpretation of the thermal data the installation details described in reference 3 should be considered. From laboratory tests of air and skin thermocouple installations which were similar to those used on the B-17F airplane, it was found that under dry-air conditions the maximum error indicated for the air temperatures was  $\pm 3^{\circ}$  F and the error of the skin temperatures was from  $0^{\circ}$  to  $8^{\circ}$  F.

The wing outer panels from stations 19A to 33 were free from ice formations during all the icing conditions encountered. Ice formed on the wing-tip leading edges during all the icing flights. The unheated landing-light cover and the leading edge at the wing splice accumulated ice as shown in figure 16. Figures 17 and 18 are photographs of the right and left wing inner panels and illustrate the partial protection afforded the right wing inner panel, between nacelles 3 and 4, by the ice-prevention system.

The heating installation for the carburetor and intercooler air inlets for nacelle 4 was not satisfactory. All the air inlets located in the wing leading edge and the elbow in the ducts from the carburetor and intercooler inlets, visible from the inlet, accumulated ice. (See figs. 19, 20, and 21.) During the flights in icing the operation of the engines did not appear to be affected by the observed icing of the inlets.

The ice-prevention system in the empennage prevented severe accumulations of ice, but several regions on the heated leading edge and aft of the heated portion of the vertical and horizontal stabilizers were not adequately heated to provide complete protection during all icing conditions encountered, as shown in figures 22 to 30. The report of the pilots indicated that the ice accumulations did not noticeably affect the stability or the control of the airplane during flight in the icing conditions.

The partial protection afforded the pilot's windshield by the temporary heating system is illustrated in figures 31 to 34. The lower portion of the windshield was protected at all times, as shown in the figures, and provided a clear area for the pilot's use. Observations of the icing of the windows during flight are presented in tables V and VI.

The heating provided for the heat-exchanger inlets prevented ice formation during all except the most severe icing conditions.

Ice accumulations on unprotected surfaces of the airplane are shown in figures 35 to 46. The unheated portions of the wing leading edge, the engine cowls, the front of the fuselage, the upper and ball gun turrets, and the housings for the fuel booster pumps and the loop antenna accumulated ice. Formations of ice were also observed during the more severe conditions on the fuselage brazier-head rivets aft of the radio compartment, and on the running and identification lights on the dorsal fin.

Several small cracks were found at the forward end of the heat exchanger which was installed in nacelle 1. This was the only evidence of failure observed when the ice-prevention system was inspected after testing had been completed.

## DISCUSSION

The test airplane was flown in icing conditions for a total of  $9\frac{3}{4}$  hours. The ice-prevention equipment provided sufficient protection to allow extended flights to be made in all icing conditions encountered. Icing was encountered at temperatures of  $-1^{\circ}$  to  $13^{\circ}$  F and  $20^{\circ}$  to  $30^{\circ}$  F, and at a maximum altitude of 12,000 feet. The maximum altitude at which thermal data were obtained was 9500 feet.

The susceptibility of unprotected surfaces of the airplane to icing is illustrated in figures 20, 27, 33, 42, and 43. The ice accumulations shown resulted from limited flight in icing conditions and indicate the necessity of providing protection for airplanes to be flown in inclement weather.

During tests 4 and 5, in which the most severe icing conditions were encountered, a 20- to 25-mile-per-hour decrease in indicated airspeed was observed for a constant engine power condition. This decrease in airspeed was not only evidenced by the airspeed indicator, but also by a decrease of the air-flow rate through the ice-prevention system, which resulted in an observed increase of the heated-air temperature. It is probable that the ice accumulations on the unprotected or insufficiently heated parts of the airplane caused this decrease in airspeed.

#### Wing Outer Panel

The ice-prevention equipment for the wing outer panel from stations 19A to 33 consisted of corrugated sheets attached to the outer skin which directed the heated air against the inner face of the wing skin. The corrugated sheets, separated at the leading edge to provide an opening for the heated air to enter the chordwise passages, terminated at approximately 15 percent of the wing chord. After flowing through the chordwise passages the heated air passed into the interior of the wing and discharged through the aileron gap.

Visual observations made during flight and immediately after landing indicated that the wing outer panel was protected from ice accumulations at all times during the tests. It was not possible to obtain any photographs of the condition of the wing outer panel during flight; however, an example of ice formation on an unheated region of the wing leading edge, which was accumulated during test 7, is shown in figure 16. This ice formation is on the right landing-light cover and extends over the unheated leading edge at the wing splice. The heated leading edge may be observed to be completely clear of ice. The heating equipment was frequently employed during take-off and climb without visible damage to the wing structure or heating equipment.

Thermal data for the wing outer panel, taken during five flights in icing conditions and two flights in dry air, are given in table III. During the flights in icing conditions the maximum structure temperature observed was 124° F, corresponding to a temperature rise above ambient air of 100° F. The highest structure temperature observed, 162° F, or 122° F above ambient air temperature,



was recorded during previously reported dry-air flights in the vicinity of Moffett Field, Calif., (reference 3) for level flight at 10,000 feet pressure altitude when the temperatures of the heated and ambient air were higher than for any condition encountered during the testing in the vicinity of Minneapolis, Minn.

The design of the ice-prevention system was based upon a spanwise air temperature drop of  $40^{\circ}$  F. For the icing flights the average spanwise air temperature drop between stations  $22\frac{1}{2}$  and 33 was  $49^{\circ}$  F and for the dry-air flights was  $34^{\circ}$  F. The reversal of the spanwise gradient of the heated air and skin temperatures between stations  $22\frac{1}{2}$  and 20 was probably due to the method by which the heated region between stations 20 and 21 was supplied with heated air (fig. 3).

The average wing outer-panel skin temperature rise forward of the 15-percent-chord point varied from approximately  $50^{\circ}$  to  $70^{\circ}$  F for the flights in icing conditions, and was approximately  $80^{\circ}$  F for the flights in dry air. It was observed that the lowest value of the average temperature rise of the wing outer-panel leading edge was obtained in the most severe icing conditions (tests 4 and 5). The data for these tests indicate that the increase of engine power resulted in a  $5^{\circ}$  F increase of the average skin temperature rise of the forward 15 percent of the wing outer panel.

An approximation of the heat flow through the forward 15 percent of the wing outer-panel skin was determined from the average air temperature drop through the chordwise passages and the air-flow rate to the wing outer panel. The approximate heat flow through the skin per square foot of wing leading-edge surface, the difference between the average temperature of the heated air in the corrugations and the ambient air temperature, and the average velocity of the air passing through the chordwise passages are presented for tests 3, 4, 5, and 7.

Test number	3	4	5	7
Heat flow through wing leading-edge surface, Btu/(hr)(sq ft) . . . . .	1200	1180	1470	1210
Difference, average air temperature in corrugations and ambient air, °F . . . . .	129	116	115	139
Average velocity of air in corrugations, ft/sec . . . . .	60	55	65	56

The data recorded during flight in icing conditions (tests 3, 4, and 7) indicate that the wing outer panel was protected with a total heat flow through the wing leading-edge surface of approximately 82,000 Btu per hour, which was approximately 50 percent of the total heat supplied to the leading-edge system and provided an average skin temperature rise forward of the 15-percent-chord point of from 50° to 70° F. The total heat flow through the wing leading-edge surface was practically constant for the same engine power conditions during the dry-air and icing flights, but the skin temperature rise was 10° to 30° F greater during the dry-air flights than during the icing flights.

#### Wing Tip

The heated air for the wing tip was obtained from the interior of the wing outer panel after flowing through the leading-edge chordwise passages. The air entered a gap between the wing skin and an added outer skin through holes in the leading edge of the inner skin and discharged at the end of the double-skin region on the upper and lower wing surfaces (fig. 4).

The protection afforded by the wing-tip system was not sufficient to prevent the formation of ice on the leading edge. Accumulations of ice were observed on the

wing tips during every flight in icing conditions. The thermal data obtained for the wing tip, given in table III, indicate that the average skin temperature rise of the heated leading-edge surface was approximately 20° F during the icing flights and 35° F during the dry-air flights.

The previously reported tests of the ice-prevention system (reference 3) indicated that the protection provided for the wing tips might be inadequate, but the urgency of testing the equipment in icing conditions prevented altering the system. It is probable that the use of air which had first been passed through the wing leading-edge system and the absence of ducting to direct the air to the wing-tip leading edge were responsible for the failure of the ice-prevention system to protect the wing tips.

#### Wing Inner Panel

The ice-prevention system for the wing inner panel consisted of an inner skin attached to the wing skin extending over the forward 4 percent of the leading edge, top and bottom, to direct the heated air against the inner face of the wing skin. The heated air was admitted into the gap between the outer and inner skins at the lower surface of the wing and was discharged into the wing interior at the gap outlet on the upper surface. The supply of heated air for the right wing inner panel was obtained from the heat exchanger in nacelle 3. The left wing inner panel was revised in the same manner as the right wing, but was not connected to a supply of heated air, pending the possible installation of a heat exchanger in nacelle 2. Protection was not provided for the oil-cooler inlets located in the wing inner-panel leading edge adjacent to the engine nacelles.

The upper surface of the wing inner panel was visible during flight, and light accumulations of ice were observed in this region during tests 4, 5, and 7. Figure 17 is a photograph of the heated region of the wing inner panel visible during test 7. Most of the ice accumulation shown has formed on the oil-cooler inlet for engine 4 and not on the heated region of the wing leading edge. The oil-cooler inlet was observed to accumulate ice during every flight in icing conditions. Figure 18 shows the unheated wing inner panel between nacelles 1 and 2

during the flight when figure 17 was obtained. A comparison of these two figures illustrates the degree of protection afforded by the heating system in the right wing inner panel.

The air temperature at the entrance to the double-skin region and at the heated-air exit gap, and the skin temperatures at one wing station are given in table IV for the heated wing leading edge between nacelles 3 and 4. The skin-temperature data indicate a considerable chordwise temperature drop from the lower to the upper surface of the heated region, in the direction of air flow, varying from approximately 70° to 110° F. The average value of the skin-temperature rise varied from 35° to 65° F, the lowest values being obtained during the most severe icing conditions (tests 4 and 5).

The degree of protection afforded by the test installation indicates that this design may prove satisfactory if the gap between the outer and inner skins was increased or tapered in order to decrease the heat lost by the air to the wing lower surface. The application of an installation similar to that employed in the wing outer panel would insure a more satisfactory temperature distribution, and although it might involve installation difficulties not encountered in the test airplane, the resulting system would be superior.

#### Carburetor and Intercooler Inlets

An experimental ice-prevention installation was provided for the lower lips only of the carburetor and intercooler air inlets for engine 4. Heated air was directed against the lower edges of the inlet openings through flattened outlets of a 1-inch-diameter branch from the supply duct to the wing outer panel.

The heated inlets were not visible to the flight personnel during flight, but ice accumulations were observed on these inlets after landing, similar to the formations shown in figure 19, which is a photograph of the intercooler air inlet for engine 1. Figures 20 and 21 show further examples of ice accretions on the air inlets. An accumulation of ice in the elbow of the ducts leading from the air inlets in the wing leading edge to the engines was observed after most of the icing flights. The most severe accumulations were observed after landing

from test 7, at which time figure 19 was obtained and shows ice on the turning vanes in the duct elbow, aft of the inlet. During flights ice was observed to accumulate on the inlets of the oil coolers to the extent that the inlet area was decreased to approximately one-half the normal area. The ice accumulated on the inlets did not appear to affect the operation of the engines during the reported limited flights in icing conditions. However, during extended operation in inclement weather, it is probable that the inlets may become sufficiently obstructed with ice to prevent desired oil cooling and eliminate the carburetor and intercooler inlets as a source of air.

The instrumentation of the heated carburetor and intercooler inlets for engine 4 consisted of one thermocouple on the lower edge of each intake. The skin temperatures recorded during flight indicate a temperature rise of approximately  $20^{\circ}$  to  $40^{\circ}$  F during icing conditions, and  $30^{\circ}$  to  $40^{\circ}$  F in dry-air conditions (table III).

The results of the flight tests indicate that the experimental heating system provided for the carburetor and intercooler inlets of engine 4 was unsatisfactory. It is probable that an installation which provides for directing heated air against the entire inlet, instead of the lower portion only, to achieve a skin temperature rise comparable to that maintained on the leading-edge surface of the wing outer panel, will prevent the accumulation of ice on the inlets.

#### Horizontal Stabilizer

The ice-prevention installation on the horizontal stabilizer utilized an outer skin attached to the stabilizer skin to provide a passage for heated air. The air entered the gap between the inner and outer skins through holes in the leading edge of the inner skin, and was discharged at the end of the double-skin region on the upper and lower surfaces of the stabilizer. The design of the horizontal stabilizer ice-prevention system was based upon a heated-air temperature of  $250^{\circ}$  F and an average skin temperature rise of  $90^{\circ}$  F at an altitude of 18,000 feet. As reported in reference 3 these design values were not realized during the tests of the equipment at Moffett Field, Calif., but in view of the limited time available for completion of the installation, the system was not altered to meet the design specification.

During all the icing flights the heating system prevented the accumulation of ice on the major portion of the heated region. The areas of the leading edge which were not adequately protected to prevent the accumulation of ice during all conditions were at the tip, at midspan, and about 10 inches of the leading edge at the junction of the horizontal stabilizer and fuselage. The extent to which the horizontal stabilizer accumulated ice is shown in figures 22, 23, and 24. In the most severe icing conditions (tests 4 and 5) ice was observed to form on the aft region of the heated double-skin and on the upper and lower surfaces of the horizontal stabilizer aft of the heated leading edge (figs. 23, 24, and 25).

Figure 26 is a photograph of the left horizontal stabilizer showing ice formation on the tip, which was the only part of the stabilizer to accumulate ice during test 7. Figure 27, a photograph of ice formation on the right horizontal stabilizer tip taken after landing from test 7, shows the ice formation extending beyond the heated portion of the leading edge almost to the point of tangency with the air flow. Ice accumulated on the extreme tips of the stabilizer during every flight in icing, indicating that the heated region should be extended completely around the forward facing curve of the tip.

The ice formations which accumulated on the leading edge of the horizontal stabilizer were found to be at the inboard, midspan, and tip regions where the distribution duct had been discontinued and the heated air discharged into a chamber through a 1-inch-diameter hole in the end of the duct (fig. 6). The thermocouples which indicated the leading-edge skin temperatures were located in or near the regions where ice accumulated and, therefore, may not give a true indication of the temperature rise of the protected portion of the leading edge. The thermal data, given in table IV for the horizontal stabilizer, show an average skin temperature rise for the leading edge of approximately  $30^{\circ}$  F for tests 1, 3, 4, and 5, and  $65^{\circ}$  F for test 7. During the dry-air flights (tests 2 and 6) the average skin temperature rise was approximately  $40^{\circ}$  F. The increase in engine power conditions (test 5) did not materially affect the skin temperature rise or the degree of protection afforded by the ice-prevention system. The heated-air flow rate to the horizontal stabilizer was not obtained, but the total weight of air supplied to the empennage group was determined and the distribution of the air to the horizontal and vertical stabilizers was based upon the skin temperature rises.

The protection of the horizontal stabilizer probably would be improved by an increase in the quantity of heat supplied and an alteration of the distribution system at the tip, midspan, and inboard sections of the leading edge to conform to the system used in the protected regions.

### Vertical Stabilizer

The vertical stabilizer leading edge was heated in a manner similar to the horizontal stabilizer. Heated air was admitted into a gap, formed by the vertical stabilizer skin and an added outer skin, through holes in the leading edge of the inner skin and discharged from the gap at the end of the double-skin region on both sides of the stabilizer. The dorsal and fin systems were essentially separate, being divided at their junction which was not provided with a double skin (fig. 7).

In the preliminary dry-air tests of the ice-prevention equipment, reported in reference 3, it was found that the heating of the vertical stabilizer was below the design value, but not to a serious degree. The results of the flight tests in icing indicate that three small areas of the leading edge were not sufficiently heated. The unsatisfactorily protected regions of the vertical stabilizer are shown in figures 28, 29, and 30, which were obtained during icing flights of tests 4, 5, and 7. The ice on the leading edge at a point approximately midway between the base and the top of the vertical stabilizer is in the vicinity of the dorsal and fin junction. Ice formations aft of the heated leading edge, which are visible on both sides of the vertical stabilizer in figures 28 and 29, were observed only during the most severe icing conditions of tests 4 and 5. The increase in engine power for test 5 did not produce any apparent change in the degree of protection afforded by the ice-prevention system for the vertical stabilizer.

The brazier-head rivets in the forward portion of the dorsal and top of fuselage, and the lights in the dorsal leading edge accumulated ice as shown in figures 28, 29, and 30. These ice accumulations probably contributed to the decrease in airspeed recorded during tests 4 and 5. Although the heating of the entire leading edge of the dorsal seems impractical, figure 29 illustrates the desirability of extending the heated double skin at least 1 foot farther forward on the dorsal.

The thermal data for the vertical stabilizer, given in table IV, indicate that the heat distribution along the leading edge was not satisfactory. The average leading-edge skin temperature rise for tests 3, 4, and 5 varied from approximately 40° F on the dorsal to 10° F on the fin tip and for test 7 from 60° F on the dorsal to 20° F on the fin tip. For the dry-air flights, tests 2 and 6, the average skin temperature rise was approximately 50° F on the dorsal and 15° F on the fin tip. During all tests the highest skin temperature rise was recorded at the lowest measuring station on the fin leading edge. The air-flow rate to the vertical stabilizer was not obtained, but the total amount of heated air supplied to the empennage was determined.

The heating of the fin tip might be improved by eliminating the bypass duct in the fin distribution system and utilizing the leading-edge duct system throughout. An increase in the quantity of heat supplied to the vertical stabilizer probably would prevent the accumulation of ice aft of the leading edge and provide protection for the leading edge at the dorsal and fin junction.

#### Windshield

The pilot's heated windshield, adapted from the service windshield and defrosting system, was protected from ice accumulations on the lower portion, as shown in figures 31 and 32. Figure 33 is a view of the windshield exterior, obtained from the aft top window of the bombardier's compartment during test 3, and illustrates the susceptibility of the windshield to icing. Although the pilot's windshield was not completely protected during flight in icing conditions, it was observed to clear more rapidly than did the unheated copilot's windshield when the airplane was flown out of the icing conditions, as shown in figure 34.

Visual observations of the windshield during tests 3, 4, and 5 are presented in tables V and VI. The average temperature of the heated air supplied to the windshield was approximately 180° F, and several measurements of the air at the outlet gap indicated an average temperature of approximately 120° F.

Although an increase in the quantity of heated air supplied to the pilot's windshield might have provided



more complete protection, the results of the test indicate that the adaption of the service windshield and defrosting system would not produce an installation which would be satisfactory for all icing conditions. It is probable that, by decreasing the gap between the two panes of glass, a satisfactory heated windshield might be developed which utilizes the same source of heated air as did the reported temporary installation.

### Windows

The pilot's windshield was the only window provided with a system to prevent accumulation of ice. The bomb-sight window was a double-pane installation similar to that originally provided for the pilot's windshield, with a defroster located at the base of the window to direct heated air against the inner face of the inner pane of glass. Observations were made of the windows to determine the susceptibility to icing. The results of observations made during tests 3, 4, and 5 are given in tables V and VI. The icing of the bomb-sight window was, in most cases, so intense that vision was completely obstructed. During the tests the upper and ball gun turrets were positioned with the sighting windows aft, and, therefore, the ice accumulations noted are on the back of the turrets. These observations have been included because they show the amount of ice which may accumulate on the forward region of the turret. The ice accumulations noted on the gun turrets in tables V and VI probably would have obstructed vision completely if the gun-sight windows had been facing forward. The scattered icing on the windows of the waist hatches and the tail gunner's compartment was not as severe as the icing observed on the bomb-sight window and on the upper and ball turrets, but was sufficient to interfere with unobstructed vision through these regions.

Photographs of the ice remaining on the upper gun turret, on the ball turret, and on the front of the fuselage, after landing from flight test 7, are presented in figures 35, 36, and 37, respectively. During flight, the ice extended over a greater area of the regions than is shown in the figures, but some of the ice was lost after leaving the icing condition. The results of these observations indicated that protection should be provided for the windows used by the gunners, the bombardier, and the pilot if the airplane is to be successfully flown in inclement weather.

### Engine Cowls

The unprotected leading edge of the engine cowls accumulated ice during all tests. The icing of the cowls during flight may be seen in figures 38 and 39, which were taken during test 3, and in figure 40, taken during test 7. The upper portion of the leading edge of the cowls did not accumulate as much ice as did the lower portion. It appeared that the engine heat provided partial protection for the engine cowls. A heating system designed to utilize the engine heat probably would provide complete protection for the engine cowls.

### General

In addition to the wing, empennage, fuselage, and engine cowls, unprotected objects, such as the airspeed-head support masts, the housings for the loop antenna and the fuel booster pumps, and the drift sight were observed to be subject to icing. Figure 43 is a photograph of ice formations accumulated during test 7 on the drift sight, the loop-antenna housing, and the left airspeed-head support mast. The ice accumulations observed on these unprotected protrusions and on the rivets and running lights (figs. 28, 29, and 30) illustrate the extreme importance of aerodynamic cleanness.

The severity of icing on the airspeed-head support mast is shown in figure 44. This figure is a photograph of the right airspeed-head mast taken at the same time figure 43 was obtained. The static-pressure openings in the airspeed head are located about  $2\frac{1}{2}$  inches forward of the support-mast leading edge. The ice accumulation shown in the figure extended to within  $1/8$  of an inch from the static openings, and is an example of the ice formation accumulated during many of the flights. An accumulation of this magnitude was found to affect the airspeed reading as much as 20 miles per hour at cruising-power conditions.

No attempt was made to prevent the accumulation of ice on the radio antennas. In figures 28, 29, and 30 ice formations may be seen on the antenna wire of the command radio. The rubber-covered steel cable which was installed in place of the service lead-in wire for the liaison radio accumulated ice as shown in figure 45. The scattering of ice on the antenna in figures 28, 29, and

30 was caused by vibrations of the wire, which broke up the accumulation. The lead-in wire for the liaison radio did not vibrate as much as did the command-radio antenna and, therefore, the ice formation on this wire was only slightly broken up. (See fig. 45.) Ice formations on the command-radio antenna were never as severe as the accretions on the liaison-radio antenna lead-in wire, which may be attributed to the fact that the liaison-radio antenna lead-in wire was approximately  $45^{\circ}$  F to the slipstream and the command-radio antenna was approximately parallel to the slipstream.

Ice which accumulated on the radio antennas did not interfere with the operation of the radio. The metal shields installed forward of the lead-in antenna insulators (fig. 46) prevented ice from forming on the insulators, and both the command-radio antenna and the liaison-radio antenna lead-in wires successfully carried the maximum ice formations which accumulated during the flights.

Figure 45 shows the ice-indicating strut which was mounted on the left side of the fuselage at the aft edge of the radio-compartment window. The ice formation on the strut leading edge was accumulated during test 7. Another illustration of icing on the strut is shown in figure 46. The ice formations shown on the strut illustrate the amount of ice which may accumulate on unprotected surfaces during flight in icing conditions. The variation in thickness of the ice on the strut probably was due to interference of the fuselage.

The two-position control valves for directing heated air into the ice-prevention system or overboard after passing through the heat exchangers failed to operate during many flights due to a mechanical failure of the valve plate and linkage mechanism. Inspection revealed that the control motors operated satisfactorily, but did not actuate the valves because of the mechanical failure of the linkage to the valve plates. A more rigid construction of the valve assemblies probably would have prevented this failure.

The exhaust-gas-to-air heat exchangers used in the tests were extended surface-fin type manufactured for the ice-prevention installation by the Stewart-Warner Corporation, and are described in reference 3. The heat exchangers were inspected during the testing at the Ice Research Project and no indications of failure were observed. After completion of tests the airplane was

returned to the AAL. An inspection revealed a failure at the forward end of the heat exchanger in nacelle 1. When the inspection was made, the exchangers had been tested for a total of 70 hours, the last 15 hours having been added after the final inspection at the Ice Research Project. This observed failure of the heat exchanger consisted of several circumferential cracks in the wall at the forward end. Discoloration of the metal indicated that the exchanger had not been sufficiently cooled in the region where the cracks occurred. Since no signs of failure were observed on the heat exchangers installed in nacelles 3 and 4, which were tested for the same length of time as was the exchanger in nacelle 1, it is believed that satisfactory distribution of cooling air would have prevented the failure of the exchanger installed in nacelle 1.

#### CONCLUSIONS

The following conclusions are based on the results of the reported flight tests of the thermal ice-prevention equipment installed on the B-17F airplane:

1. In all parts of the ice-prevention equipment where the design specifications were realized, they were demonstrated to be satisfactory and should prove adequate for any similar installation. Where the design specifications were not satisfied, the system failed to prevent completely the formation of ice.

2. The results of the reported flight tests further substantiated the fact that sufficient data are available for the design of thermal ice-prevention equipment for airplanes which will provide protection from icing.

3. Ample heat for ice prevention may be supplied without apparent deleterious thermal effects on the wing structure.

Ames Aeronautical Laboratory,  
National Advisory Committee for Aeronautics,  
Moffett Field, Calif.

## REFERENCES

1. Rodert, Lewis A., Clousing, Lawrence A., and McAvoy, William H.: Recent Flight Research on Ice Prevention. NACA ARR, Jan. 1942.
2. Jones, Alun R., and Rodert, Lewis A.: Development of Thermal Ice-Prevention Equipment for the B-24D Airplane. NACA ACR, Feb. 1943.
3. Jones, Alun R., and Rodert, Lewis A.: Development of Thermal Ice-Prevention Equipment for the B-17F Airplane. NACA ARR No. 3H24, Aug. 1943.

TABLE I.- FLIGHTS IN ICING CONDITIONS MADE IN THE B-17F AIRPLANE EQUIPPED  
WITH A THERMAL ICE-PREVENTION SYSTEM

Test number <sup>1</sup>	-----	1	-----	-----	3	4, 5	7
Date . . . . .	2-23-43	2-24-43	3-3-43	3-4-43	3-13-43	3-14-43	3-27-43
Time in icing condition, hr. . . . .	$1\frac{1}{2}$	$1/2$	$3/4$	$1/2$	2	2	$2\frac{1}{2}$
Ambient-air temperature range during icing, °F .	20 to 27	-1 to 10	4 to 8	9 to 11	24 to 30	24 to 30	9 to 13
Altitude range in icing, ft .	3000 to 4300	4000 to 5000 and 8000 to 10,000	4500 to 7000	6000 to 7000	3000 to 4000	4000 to 4300	9500 to 12,000
Severity of icing <sup>2</sup> . . .	2	1	1	2	3	4	2
Type of ice	Glaze	Rime	Rime	Rime	Glaze	Glaze	Rime

<sup>1</sup>For reference to tables II, III, and IV.

<sup>2</sup>Arbitrary index of icing severity; the least severe icing is designated as 1, the most severe as 4.

A-23

TABLE II.- FLIGHT AND ENGINE DATA RECORDED DURING FLIGHT TESTS OF THE B-17F AIRPLANE THERMAL ICE-PREVENTION EQUIPMENT

Test number . . . . .	1	<sup>1</sup> 2	3	4	5	<sup>1</sup> 6	7
Condition . . . . .	Level flight	Level flight	Level flight	Level flight	Level flight	Level flight	Level flight
Date . . . . .	2-24-43	2-24-43	3-13-43	3-14-43	3-14-43	3-18-43	3-27-43
Time thermal data were taken. .	3:30 p.m. to 4:00 p.m.	4:15 p.m. to 4:45 p.m.	3.00 p.m. to 3:45 p.m.	1:15 p.m. to 1:45 p.m.	2:00 p.m. to 2:30 p.m.	11:45 a.m. to 12:15 p.m.	12:00 noon to 12:30 p.m.
Location. . . . .	Green Bay, Wis.	Eau Claire, Wis.	Eau Claire, Wis.	Duluth, Minn.	Duluth, Minn.	Sioux Falls, S. Dak.	Benson, Minn.
Pressure altitude at which thermal data were taken, ft. . . .	7500 to 7100	4250	3850	4150	4000	4000	9500
Ambient air temperature, °F . .	2-3	3-5	26	21-27	23-26	17-19	12-13
Corrected indicated airspeed, mph	170-175	170	170	172-150	180-155	170	170
Manifold pressure, in. Hg.:							
Engine 1 . . . . .	27	28	27.5	28	31	28	28
Engine 3 . . . . .	27	28	28	28	31	28	28
Engine 4 . . . . .	27	28	28	28	31	28	28
Engine speed, rpm:							
Engine 1 . . . . .	1740	1740	1750	1750	2060	1640	1750
Engine 3 . . . . .	1800	1800	1800	1800	2100	1700	1800
Engine 4 . . . . .	1800	1800	1800	1800	2100	1700	1800

<sup>1</sup>Flight in dry air.





TABLE III  
RESULTS OF FLIGHT TESTS OF THE THERMAL ICE-PREVENTION EQUIPMENT  
INSTALLED IN THE RIGHT WING OUTER PANEL OF THE B-17F AIRPLANE

Thermo-couple number	Test number	1	2	3	4	5	6	7
	Pressure altitude, ft - - - - -	7500	4250	3850	4150	4000	4000	9500
	Corrected indicated airspeed, mph - - - - -	175	170	170	172-150	180-155	170	--
	Ambient-air temperature, °F - - - - -	3	4	26	24	25	18	13
	Weight of air to outboard section, lb/hr - - - - -	2540	2860	2860	2940-2420	3330-2870	2820	2160
A40	Temperature of air into No. 4 exchanger, °F - - - - -	3	4	26	24	25	18	13
A41	Temperature of air out of No. 4 exchanger, °F - - - - -	280	256	280	280-323	288-302	268	343
	Air temperature rise, °F - - - - -	277	251	254	256-299	263-277	250	330
	Heat to air, Btu/hr - - - - -	169,000	173,000	175,000	181,000 174,000	211,000 192,000	169,000	172,000
	<u>Air temperatures, °F</u>							
A7	Air into gap, sta. 20 - - - - -	185	180	198	182	186	185	208
A8	Air at upper gap exit, sta. 20 - - - - -	--	53	71	60	55	64	58
A9	Air at lower gap exit, sta. 20 - - - - -	--	53	66	56	47	64	44
A14	Air in wing near aileron gap, sta. 20 - - - - -	--	30	40	35	39	41	35
A11	Air into gap, sta. 22-1/2 - - - - -	228	220	245	243	245	231	293
A4	Air into gap, sta. 25 - - - - -	223	215	235	232	237	221	272
A5	Air at upper gap exit, sta. 25 - - - - -	--	76	93	84	79	84	76
A6	Air at lower gap exit, sta. 25 - - - - -	--	102	137	90	78	121	80
A13	Air in wing near aileron gap, sta. 24-1/2 - - - - -	--	40	47	45	47	41	41
A10	Air into gap, sta. 29 - - - - -	213	209	229	219	227	214	255
A1	Air into gap, sta. 33 - - - - -	195	190	206	192	201	193	217
A2	Air at upper gap exit, sta. 33 - - - - -	--	97	105	90	94	100	85
A3	Air at lower gap exit, sta. 33 - - - - -	--	97	107	90	85	102	85
A12	Air in wing near aileron gap, sta. 32 - - - - -	--	65	80	61	69	73	69
A28	Air into gap, wing tip, sta. 35 - - - - -	--	91	97	86	88	102	65
	<u>Skin temperatures, °F above ambient-air temp.</u>							
S76	Intercooler air-intake lip at 5% chord, sta. 15 1/2 - - - - -	--	39	21	21	27	42	35
S75	Carburetor air-intake lip at 5% chord, sta. 16 1/2 - - - - -	--	28	21	21	27	39	41
S25	On nose, sta. 20 - - - - -	110	110	60	54	66	106	71
S26	Upper at 3% chord, sta. 20 - - - - -	--	97	68	58	66	77	78
S27	Lower at 3% chord, sta. 20 - - - - -	--	93	56	42	44	91	66
S28	Upper at 8% chord, sta. 20 - - - - -	--	43	37	27	31	45	41
S29	Lower at 8% chord, sta. 20 - - - - -	--	60	40	25	25	60	40
S30	Upper at 13% chord, sta. 20 - - - - -	--	32	24	16	20	32	29
S31	Lower at 13% chord, sta. 20 - - - - -	--	36	28	12	14	37	28
S39	Upper near aileron gap, sta. 20 - - - - -	--	16	10	6	6	16	20
S20	On nose, sta. 22-1/2 - - - - -	175	173	156	119	154	164	177
S21	Upper at 3% chord, sta. 22-1/2 - - - - -	--	133	92	76	78	91	117
S22	Lower at 3% chord, sta. 22-1/2 - - - - -	--	143	124	93	113	138	129

24

S23	Upper at 12% chord, sta. 22-1/2	--	59	54	46	51	58	65
S24	Lower at 12% chord, sta. 22-1/2	--	107	60	41	43	101	64
S13	On nose, sta. 25	143	143	129	89	113	137	113
S14	Upper at 4% chord, sta. 25	129	126	119	89	97	117	110
S15	Lower at 4% chord, sta. 25	143	143	137	98	110	137	120
S16	Upper at 8% chord, sta. 25	66	66	60	49	55	63	65
S17	Lower at 8% chord, sta. 25	103	107	106	49	55	112	69
S18	Upper at 13% chord, sta. 25	52	51	47	38	43	52	49
S19	Lower at 13% chord, sta. 25	73	87	88	41	44	98	55
S52	Upper at 25% chord, sta. 24-1/2	--	27	26	16	19	30	32
S53	Lower at 25% chord, sta. 24-1/2	--	35	14	12	16	22	26
S33	Upper at 35% chord, sta. 24-1/2	--	22	19	13	18	27	31
S34	Lower at 35% chord, sta. 24-1/2	--	22	14	7	11	19	21
S54	Upper at 50% chord, sta. 24-1/2	--	17	14	12	13	23	25
S55	Lower at 50% chord, sta. 24-1/2	--	14	8	7	6	19	17
S35	Upper at 65% chord, sta. 24-1/2	--	17	14	7	11	12	25
S36	Lower at 65% chord, sta. 24-1/2	--	8	8	5	5	14	17
S37	Upper near aileron gap, sta. 24-1/2	--	13	12	6	5	21	22
S38	Lower near aileron gap, sta. 24-1/2	--	13	6	4	5	16	16
S8	On nose, sta. 29	131	127	112	79	92	122	100
S9	Upper at 3% chord, sta. 29	--	117	110	85	75	108	107
S10	Lower at 3% chord, sta. 29	--	134	128	85	101	130	98
S11	Upper at 10% chord, sta. 29	--	64	56	51	50	64	61
S12	Lower at 10% chord, sta. 29	--	106	94	52	54	104	70
S1	On nose, sta. 33	101	99	88	61	63	98	78
S2	Upper at 3% chord, sta. 33	137	133	126	92	93	126	108
S3	Lower at 3% chord, sta. 33	101	98	92	78	74	94	96
S4	Upper at 8% chord, sta. 33	67	66	60	52	52	65	62
S5	Lower at 8% chord, sta. 33	103	100	94	55	52	99	69
S6	Upper at 11% chord, sta. 33	69	65	60	48	50	66	60
S7	Lower at 11% chord, sta. 33	73	73	70	48	44	77	51
S32	Upper at 65% chord, sta. 32	--	22	19	13	18	27	28
S56	On nose, wing tip, sta. 35	31	35	25	22	19	46	22
S57	Upper, wing tip at 5% chord, sta. 35	31	35	25	21	20	43	23
S58	Lower, wing tip at 5% chord, sta. 35	14	17	11	12	7	33	12
Structure temperatures, °F								
M3	On rib at 7% chord, sta. 20	--	83	90	80	88	87	89
M2	On rib at 7% chord, sta. 25	--	110	123	110	124	118	118
M1	On rib at 7% chord, sta. 33	--	103	110	95	110	110	103

<sup>1</sup>Numbers correspond to thermocouple locations on figure 3.

<sup>2</sup>Flights in dry air.

<sup>3</sup>Measured at 5-inch venturi.

TABLE IV  
RESULTS OF FLIGHT TESTS OF THE THERMAL ICE-PREVENTION EQUIPMENT INSTALLED  
IN THE RIGHT WING INNER PANEL AND THE EMPENNAGE OF THE XB-17F AIRPLANE

Thermo-couple number	Test number	1	1 <sup>2</sup>	3	4	5	1 <sup>6</sup>	7
	Pressure altitude, ft - - - - -	75-7100	4250	3850	4150	4000	4000	9500
	Corrected indicated airspeed, mph - - - - -	175	170	170	172-150	180-155	170	--
	Ambient-air temperature, °F - - - - -	3	5	26	24	25	19	13
A42	Temperature of air out of No. 3 exchanger, °F	279	234	310	298-334	304-319	279	346
	Air temperature rise, °F - - - - -	276	229	284	274-310	279-294	260	333
	*Weight of air to empennage, lb/hr - - - - -	2200	3020	2920	2880-2600	3040-2840	2980	2420
	‡Heat to air, No. 3 exchanger, Btu/hr - - -	146,000	166,000	199,000	190,000 124,000	204,000 201,000	186,000	194,000
	<u>Wing inner-panel air temperatures, °F</u>							
A39	In duct at 4% chord, sta. 9 - - - - -	189	176	230	232	229	208	257
A38	At gap exit at 4% chord, sta. 9 - - - - -	--	41	60	54	51	55	57
	<u>Wing inner-panel skin temperatures, °F above ambient-air temperature</u>							
S74	Lower at 3-1/2% chord, sta. 9 - - - - -	103	81	104	85	70	104	131
S72	Lower at 1% chord, sta. 9 - - - - -	86	71	80	53	49	80	97
S70	On nose, sta. 9 - - - - -	67	60	57	41	43	64	60
S71	Upper at 1% chord, sta. 9 - - - - -	42	33	28	18	16	44	30
S73	Upper at 3-1/2% chord, sta. 9 - - - - -	24	8	14	2	2	23	19
	<u>Wing inner-panel structure temperatures, °F</u>							
M11	On rib at 3% chord, sta. 9 - - - - -	--	--	78	71	67	77	77
	<u>Right stabilizer air temperatures, °F</u>							
A35	Air into gap, inboard sta. - - - - -	64	60	115	122	125	88	131
A36	At upper gap exit, inboard sta. - - - - -	--	11	30	26	29	29	23
A37	At lower gap exit, inboard sta. - - - - -	--	19	49	46	50	42	43
A32	Air into gap, center sta. - - - - -	77	70	106	106	104	103	113
A33	At upper gap exit, center sta. - - - - -	--	30	56	32	31	57	73
A34	At lower gap exit, center sta. - - - - -	--	55	77	68	76	80	75
A29	Air into gap, outboard sta. - - - - -	59	56	89	85	89	86	93
A30	Air at upper gap exit, outboard sta. - - - -	--	27	45	44	42	53	45
A31	Air at lower gap exit, outboard sta. - - - -	--	27	48	44	46	55	50

<u>Right stabilizer skin temperatures, °F above ambient-air temperature</u>								
S67	On nose, inboard sta. - - - - -	27	27	27	25	27	26	53
S68	Upper near air exit, inboard sta. - - - - -	11	9	8	9	4	5	15
S69	Lower near air exit, inboard sta. - - - - -	14	15	20	20	21	10	27
S62	On nose, center sta. - - - - -	54	48	37	35	32	55	60
S63	Upper near air exit, center sta. - - - - -	27	32	26	9	9	45	44
S64	Lower near air exit, center sta. - - - - -	47	43	34	28	31	45	38
S65	Upper at 20% chord, center sta. - - - - -	--	10	8	0	4	6	14
S66	Lower at 20% chord, center sta. - - - - -	--	12	11	6	7	8	14
S59	On nose, outboard sta. - - - - -	34	41	37	50	40	60	65
S60	Upper near air exit, outboard sta. - - - - -	21	24	21	23	2	42	32
S61	Lower near air exit, outboard sta. - - - - -	34	35	26	23	31	44	32
<u>Right stabilizer structure temperature, °F</u>								
M10	On rib, inboard sta. - - - - -	--	32	66	66	65	60	68
M9	On rib, at midspan - - - - -	--	65	103	103	106	103	112
M8	On spar baffle, outboard sta. - - - - -	--	30	57	53	55	56	50
<u>Dorsal air temperatures, °F</u>								
A24	Air into gap, bottom sta. - - - - -	202	187	250	263	268	230	--
A25	Air into gap, top sta. - - - - -	124	111	174	187	196	156	200
A26	Air at left gap exit, top sta. - - - - -	--	35	52	52	56	63	54
A27	Air at right gap exit, top sta. - - - - -	--	25	48	28	33	43	39
<u>Dorsal skin temperatures, °F above ambient-air temperature</u>								
S49	On nose, top sta. - - - - -	49	48	46	42	45	59	65
S50	Left skin near air exit, top sta. - - - - -	37	35	44	14	12	33	53
S51	Right skin near air exit, top sta. - - - - -	44	45	48	52	52	56	60
<u>Dorsal structure temperature, °F</u>								
M7	On rib, top sta. - - - - -	--	82	135	139	146	122	151

(Continued on next page)

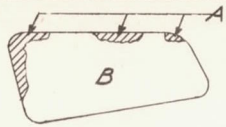
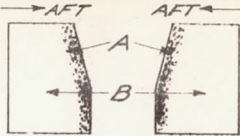
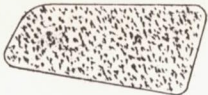

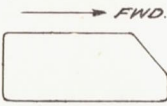
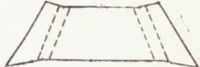


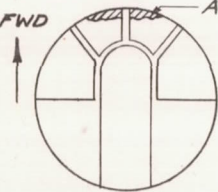
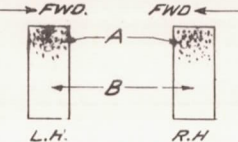
TABLE IV (Concluded)

23  
02

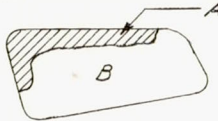
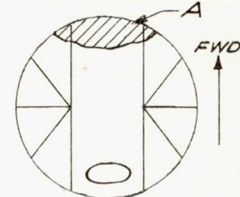
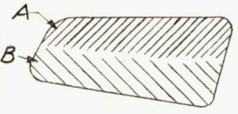
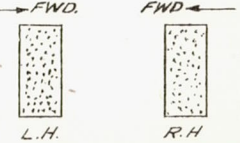
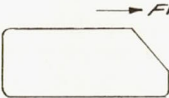
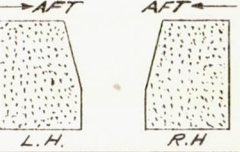

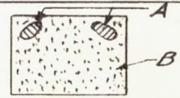
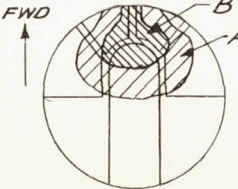
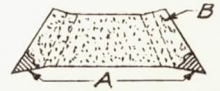
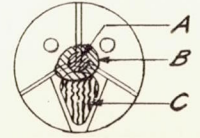
Thermo- couple number	Test number r	1	<sup>2</sup> 2	3	4	5	<sup>2</sup> 6	7
	<u>Fin air temperatures, °F</u>							
A15	Air into gap, bottom sta. - - - - -	184	169	222	235	239	--	250
A17	At right gap exit, bottom sta. - - - - -	--	74	100	39	32	85	112
A18	Air into gap, center sta. - - - - -	88	83	123	130	128	121	140
A19	At left gap exit, center sta. - - - - -	--	53	78	75	69	83	80
A20	At right gap exit, center sta. - - - - -	--	29	52	36	33	51	40
A21	Air into gap, top sta. - - - - -	25	26	52	51	56	51	57
A22	At left gap exit, top sta. - - - - -	--	16	36	32	33	37	33
A23	At right gap exit, top sta. - - - - -	--	17	44	36	43	42	43
	<u>Fin skin temperatures, °F above ambient-air temperature</u>							
S40	On nose, bottom sta. - - - - -	87	82	84	74	75	89	109
S41	Left skin near air exit, bottom sta. - - - - -	--	35	30	25	21	45	38
S42	Right skin near air exit, bottom sta. - - - - -	--	34	35	19	11	38	52
S43	On nose, center sta. - - - - -	53	48	50	36	40	61	73
S44	Left skin near air exit, center sta. - - - - -	--	40	41	36	37	48	61
S45	Right skin near air exit, center sta. - - - - -	--	30	37	22	27	42	52
S46	On nose, top sta. - - - - -	17	16	15	12	14	21	24
S47	Left skin near air exit, top sta. - - - - -	--	15	13	9	11	16	17
S48	Right skin near air exit, top sta. - - - - -	--	10	13	9	11	16	22
	<u>Fin structure temperatures, °F</u>							
M4	On spar baffle, bottom sta. - - - - -	--	32	60	69	69	52	60
M5	On spar baffle, at midspan - - - - -	--	57	92	97	95	86	103
M6	On spar baffle, top sta. - - - - -	--	18	44	43	76	40	42

<sup>1</sup> Flights in dry air.<sup>2</sup> Measured at 6-inch venturi.<sup>3</sup> Based on air flow to empennage, neglecting small amount of air flow to wing inner panel.

TABLE V  
OBSERVATIONS OF THE WINDOWS OF THE B-17F AIRPLANE DURING FLIGHT IN ICING CONDITIONS, TEST NUMBER 3.

WINDOW	OBSERVED ICING	REMARKS	WINDOW	OBSERVED ICING	REMARKS
PILOTS WINDSHIELD, TRUE REAR VIEW.		A-SOLID ICE FORMATION. B-NO ICE, KEPT CLEAR BY HEATING SYSTEM.	SIDE WINDOWS, TAIL GUN COMPARTMENT, INSIDE VIEW.		A-LIGHT, SCATTERED ICE FORMATION. B-CLEAR OF ICE.
CO-PILOTS WINDSHIELD, TRUE REAR VIEW.		ENTIRE WINDOW COVERED WITH ICE, COMPLETELY OBSCURING VISION.	GUNNERS WINDOW, TAIL GUN COMPARTMENT, FRONT VIEW.		CLEAR OF ICE.
L.H. SLIDING WINDOW IN PILOTS COMPARTMENT, INSIDE VIEW. R. H. OPPOSITE.		BOTH WINDOWS WERE CLEAR OF ICE.	PICK-UP WINDOW, TAIL GUN COMPARTMENT, FRONT VIEW.		CLEAR OF ICE.
BOMBSIGHT WINDOW, TRUE VIEW.		ENTIRE WINDOW SPECKLED WITH ICE, COMPLETELY OBSCURING VISION.	FRONT OF FUSELAGE, REAR VIEW.		A-SOLID FORMATIONS OF ICE. B-SPECKLED WITH ICE. REMAINDER CLEAR OF ICE.
UPPER GUN TURRET, TOP VIEW.		A-SOLID FORMATION OF ICE, REMAINDER CLEAR OF ICE.			
WAIST GUN WINDOWS, INSIDE VIEW.		A-LIGHT, SCATTERED ICE FORMATION. B-CLEAR OF ICE.			

**TABLE VI**  
**OBSERVATIONS OF THE WINDOWS OF THE B-17F AIRPLANE DURING FLIGHT IN ICING CONDITIONS, TESTS NUMBER 4 & 5**

WINDOW	OBSERVED ICING	REMARKS	WINDOW	OBSERVED ICING	REMARKS
PILOTS WINDSHIELD, TRUE REAR VIEW.		A-SOLID COATING OF ICE B-NO ICE. KEPT CLEAR BY HEATING SYSTEM.	BALL GUN TURRET, TOP VIEW.		A-SOLID COATING OF ICE. REMAINDER OF TURRET CLEAR OF ICE
CO-PILOTS WINDSHIELD, TRUE REAR VIEW.		SOLID COATING OF ICE ON ENTIRE WINDOW. REGION A HEAVIER THAN REGION B.	WAIST GUN WINDOWS, INSIDE VIEW.		BOTH WINDOWS SPECKLED WITH ICE.
L.H. SLIDING WINDOW IN PILOT'S COMPARTMENT, INSIDE VIEW. R H. OPPOSITE.		BOTH WINDOWS WERE CLEAR OF ICE.	SIDE WINDOWS, TAIL GUN COMPARTMENT, INSIDE VIEW.		BOTH WINDOWS SPECKLED WITH ICE.
BOMBSIGHT WINDOW, TRUE VIEW		RIDGES OF ICE, COMPLETELY OBSCURING WINDOW	GUNNERS WINDOW, TAIL GUN COMPARTMENT, FRONT VIEW.		A-FIRST OBSERVATION, TWO RIDGES OF ICE ONLY. B-LATER OBSERVATION, ENTIRE WINDOW SPECKLED WITH ICE.
UPPER GUN TURRET, TOP VIEW.		A-SOLID COATING OF ICE. B-SOLID COATING OF ICE, HEAVIER THAN A. REMAINDER OF TURRET CLEAR OF ICE.	PICK-UP WINDOW, TAIL GUN COMPARTMENT, FRONT VIEW.		A-FIRST OBSERVATION, TWO SPOTS OF ICE ONLY B-LATER OBSERVATION, ENTIRE WINDOW SPECKLED WITH ICE.
			FRONT OF FUSELAGE, REAR VIEW		A-SOLID COATING, LIGHT ICE. B-SOLID COATING, HEAVIER THAN A. C-RIDGES OF ICE, REMAINDER CLEAR OF ICE

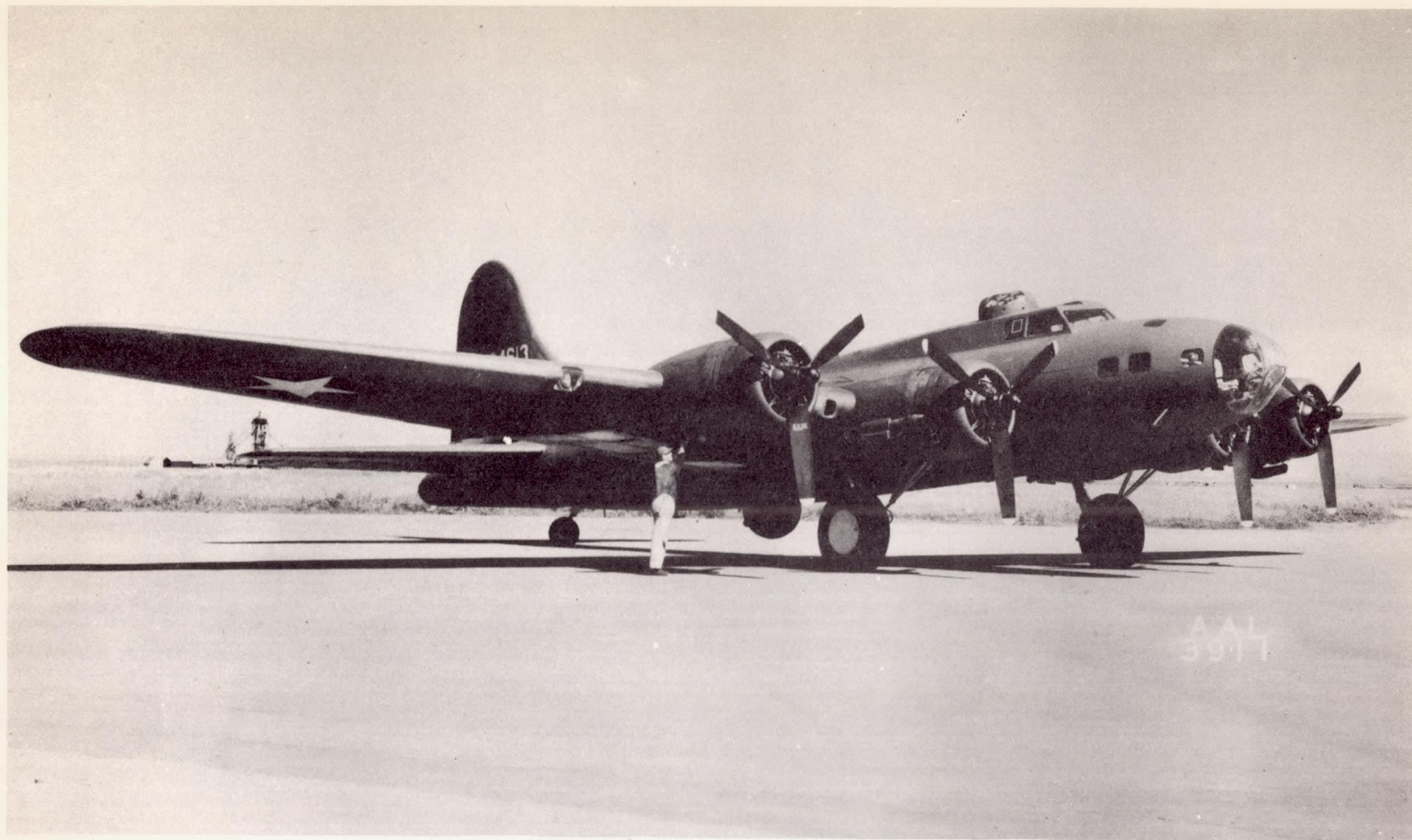


Figure 1.- The B-17F airplane in which the thermal ice-prevention equipment has been installed.



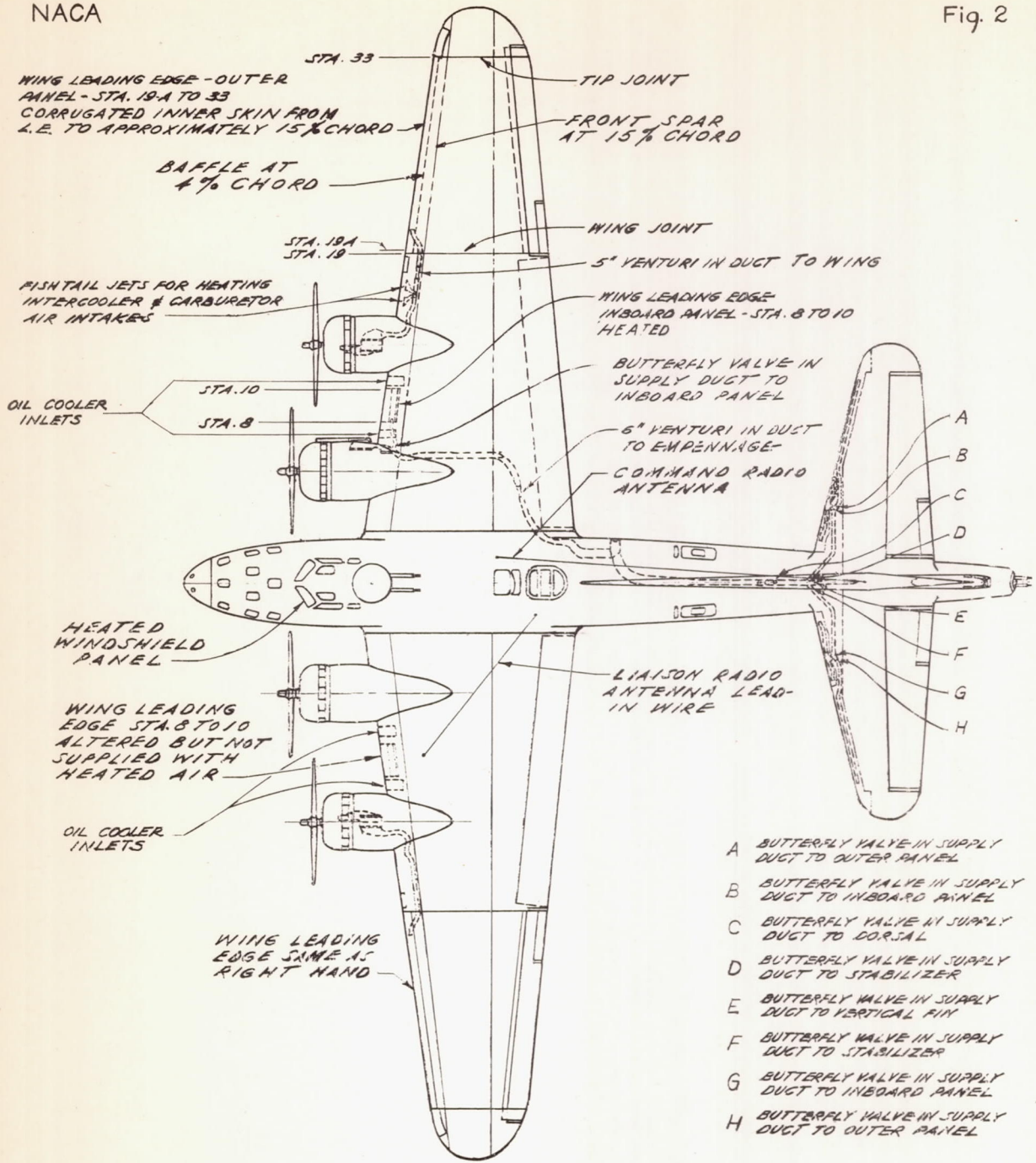


FIGURE 2.- THE THERMAL ICE-PREVENTION SYSTEM AS INSTALLED IN THE B-17F AIRPLANE.

A-23

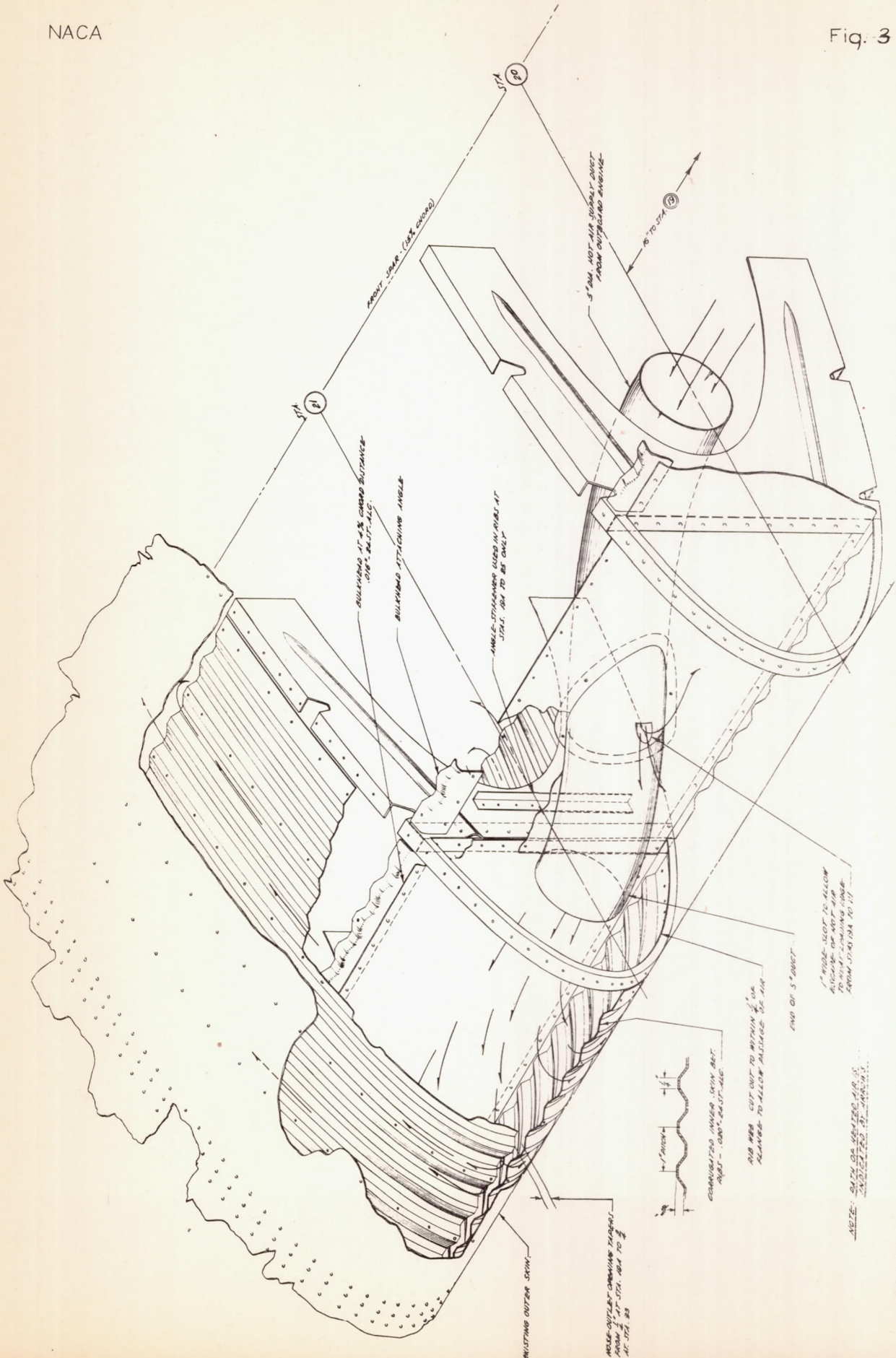
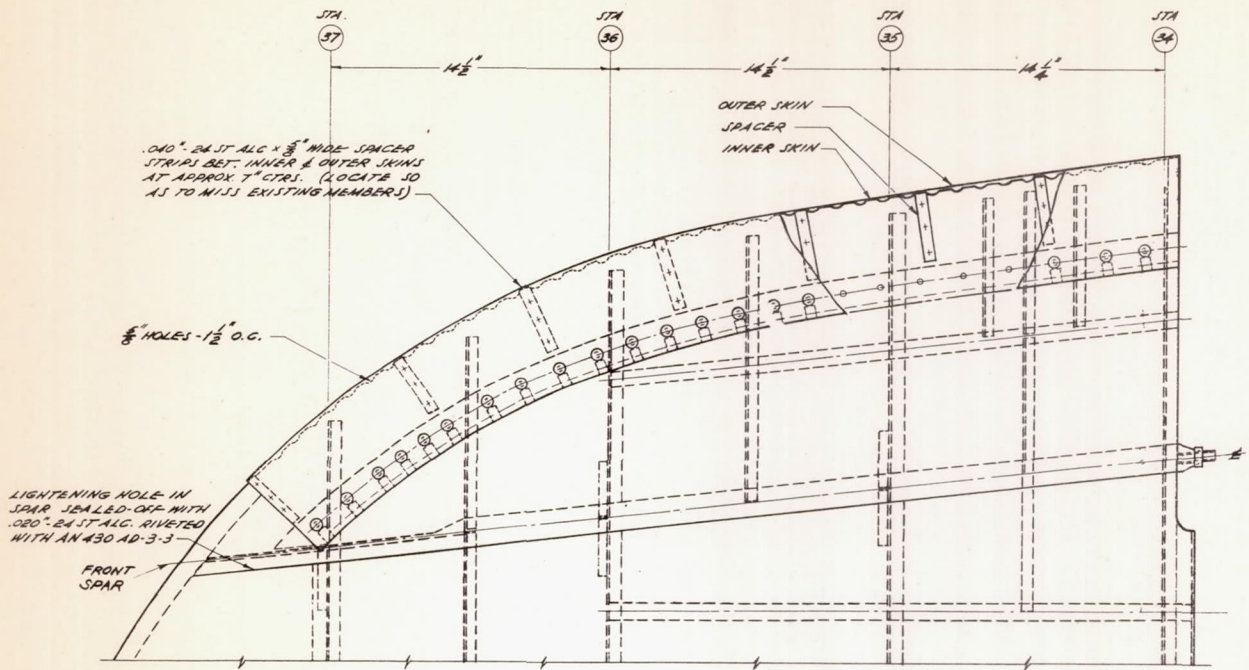
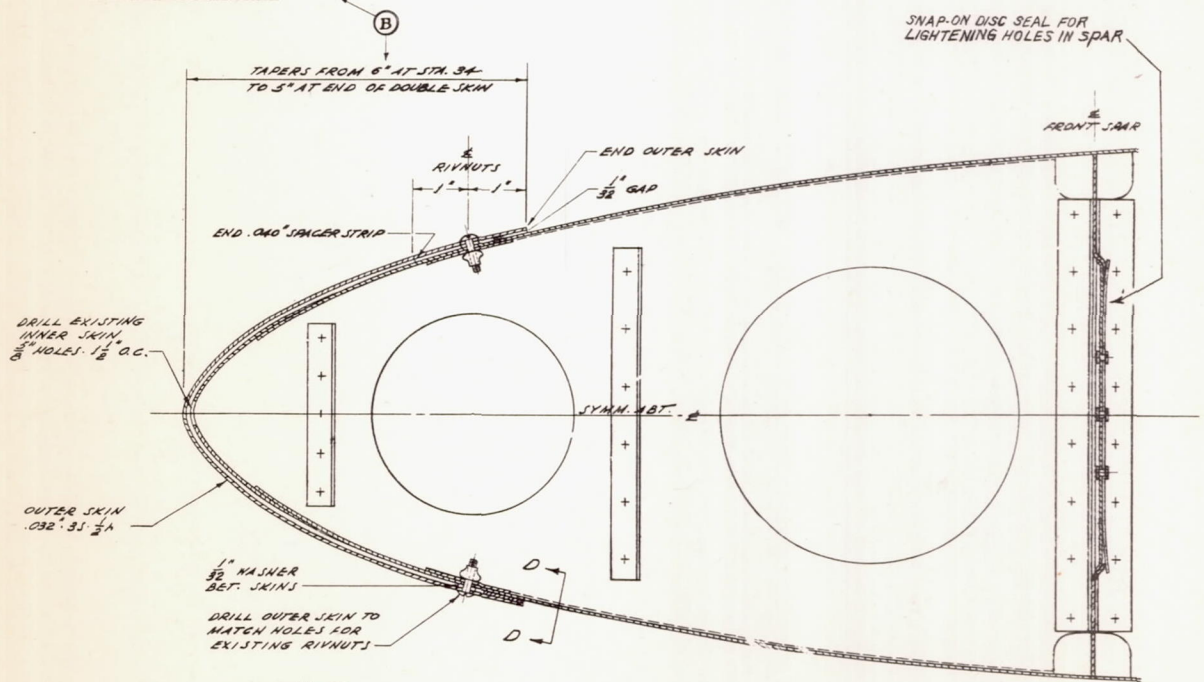


FIGURE 3 - DETAILS OF WING OUTER-PANEL LEADING-EDGE DESIGN FOR B-17F THERMAL ICE-PREVENTION SYSTEM.



NOTE:  
I.E. SPACER STRIPS ARE ATTACHED TO INNER SKIN WITH BAC1341AD3-3 APPROX 1 1/2" O.C.  
B.A.C. STANDS FOR BOEING AIRCRAFT COMPANY

LEFT WING TIP - LEADING EDGE (RIGHT WING OPP HAND)



TYPICAL SECTION THRU LEADING EDGE

NOT TO SCALE

SECT. 'D-D'

FIGURE 4.-WING-TIP DETAILS FOR B-17F THERMAL ICE-PREVENTION SYSTEM.

NACA

Fig. 5

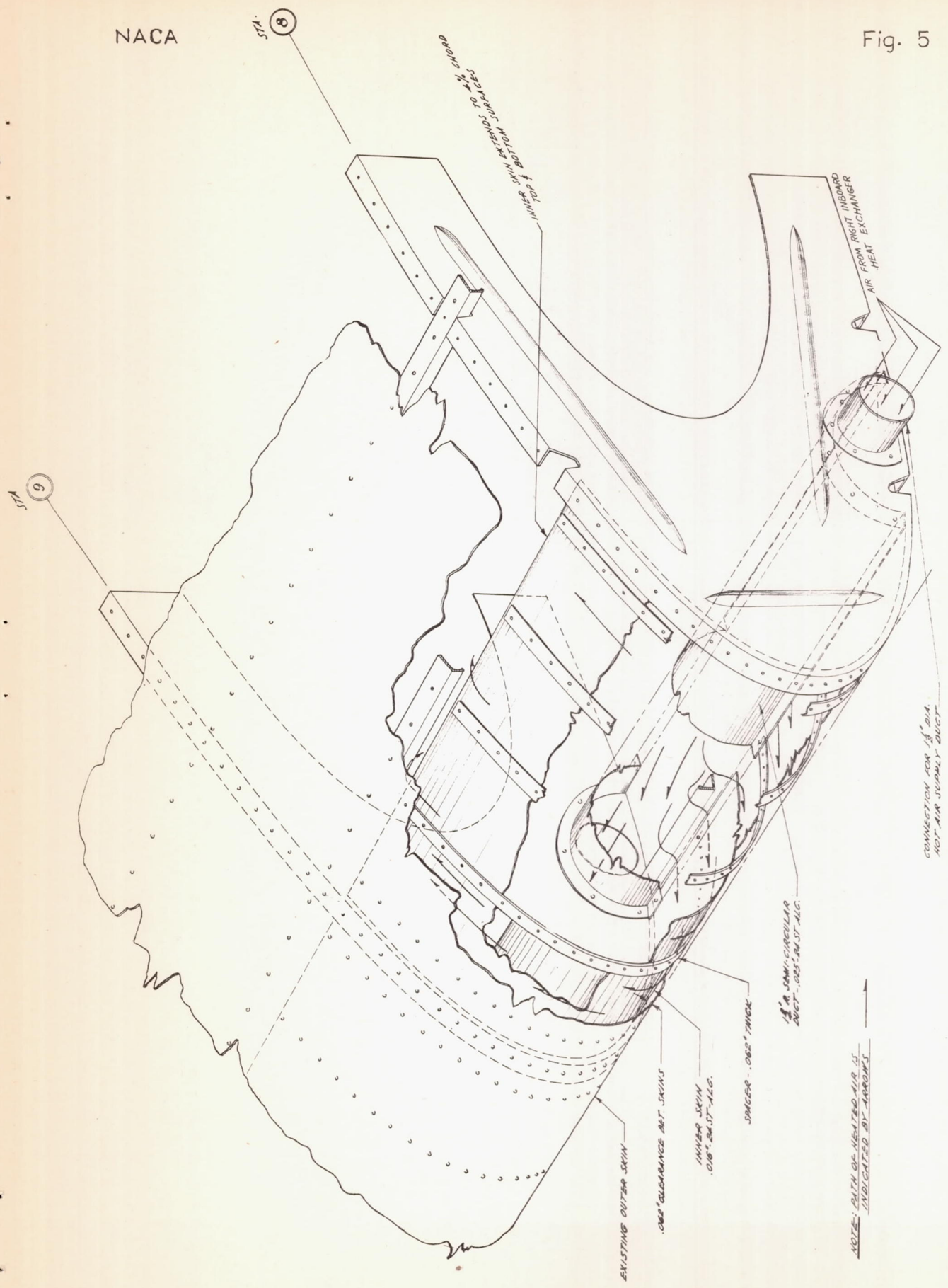


FIGURE 5-- WING INNER PANEL LEADING-EDGE DESIGN (STATIONS 8 TO 10) FOR B-17F AIRPLANE THERMAL ICE--PREVENTION SYSTEM.

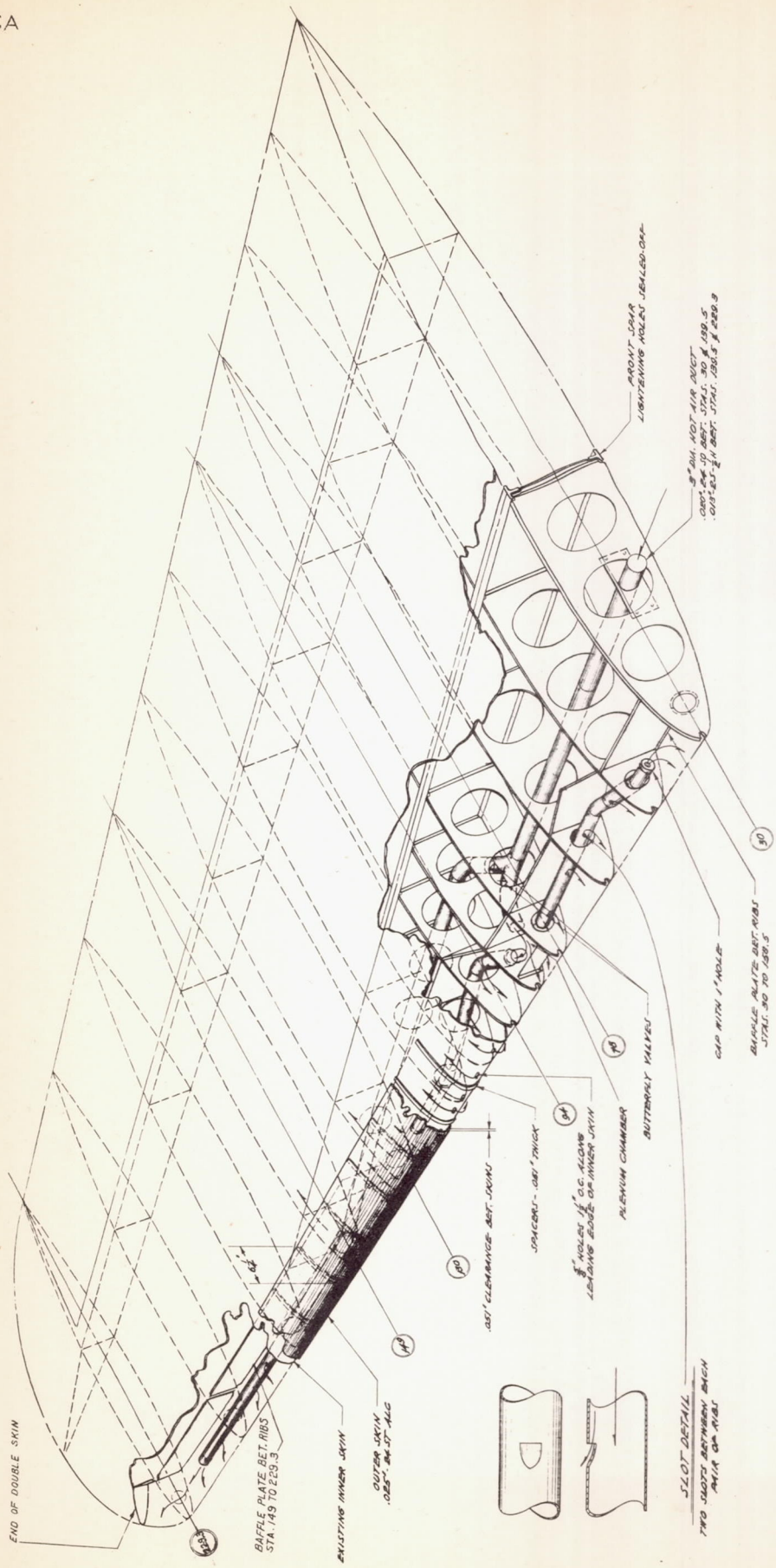


FIGURE 6.- HORIZONTAL STABILIZER DESIGN FOR B-17F THERMAL ICE-PREVENTION SYSTEM.

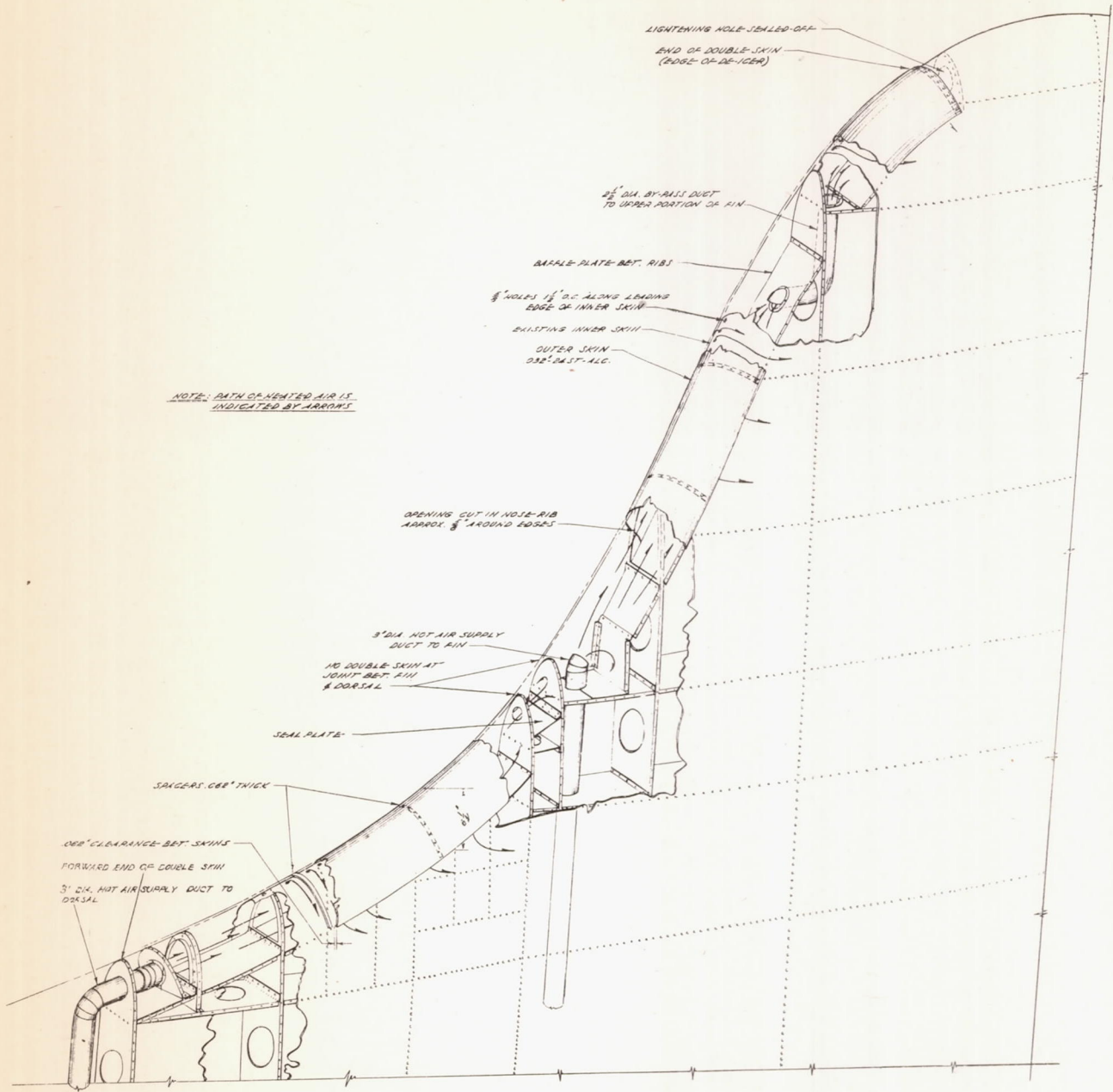
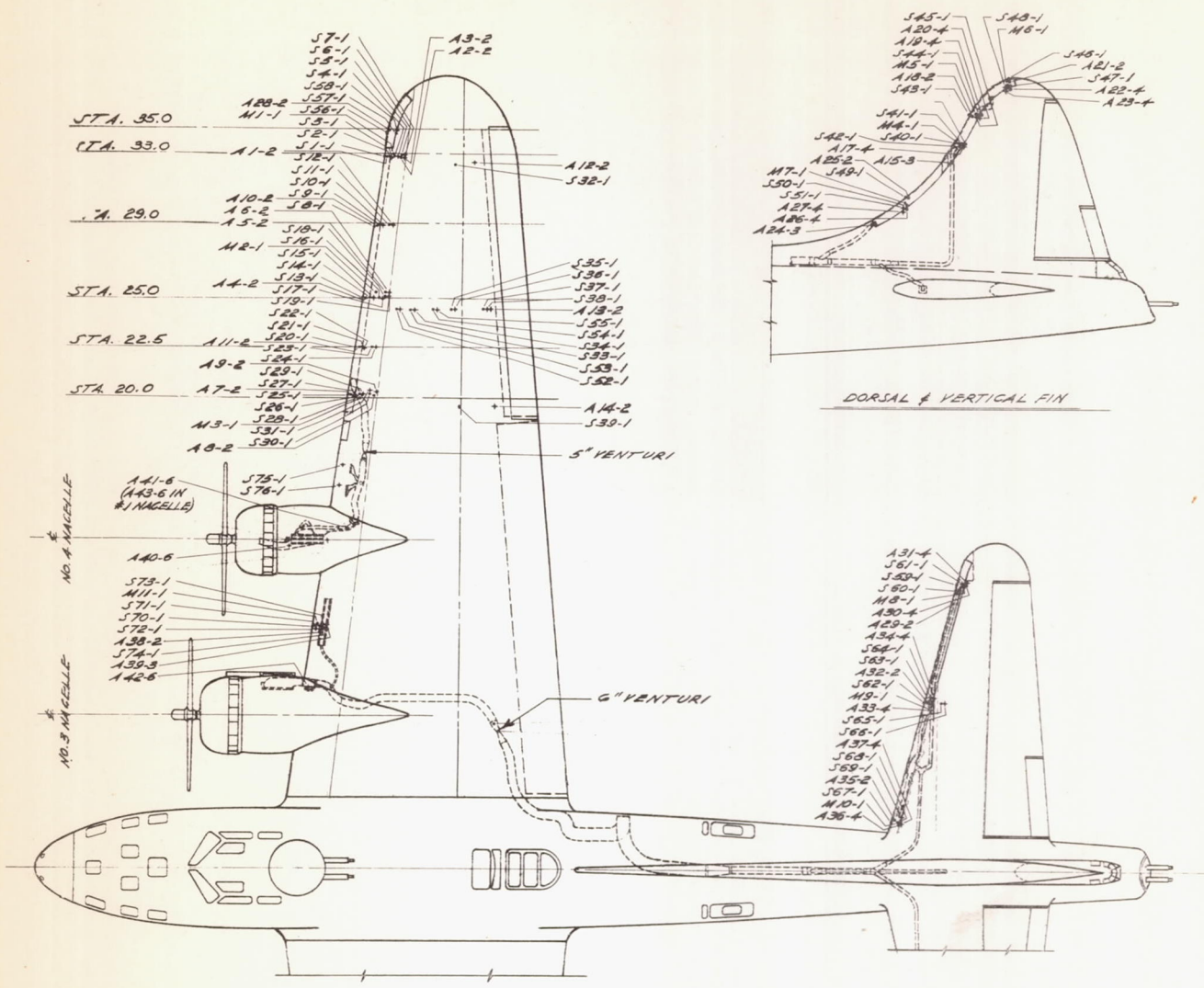


FIGURE 7.- DORSAL AND FIN DESIGN FOR B-17F THERMAL ICE-PREVENTION SYSTEM.

A-23



— LEGEND —

- A - AIR THERMOCOUPLES
- S - SKIN THERMOCOUPLES
- M - STRUCTURE THERMOCOUPLES
- - ALL THERMOCOUPLES ON OR ABOVE WING OR STABILIZER & OR ON LEFT SIDE OF DORSAL & FIN.
- ◆ - ALL THERMOCOUPLES BELOW WING OR STABILIZER & OR ON RIGHT SIDE OF DORSAL & FIN &.

NOTE: DASH NUMBERS FOLLOWING THERMOCOUPLE NUMBERS INDICATE TYPE OF MOUNTING AS DETAILED IN FIGURE 34 OF REF. 3.

FIGURE 8.-LOCATION OF THERMOCOUPLES FOR THE PERFORMANCE TESTS OF THE B-17F AIRPLANE THERMAL ICE-PREVENTION SYSTEM.

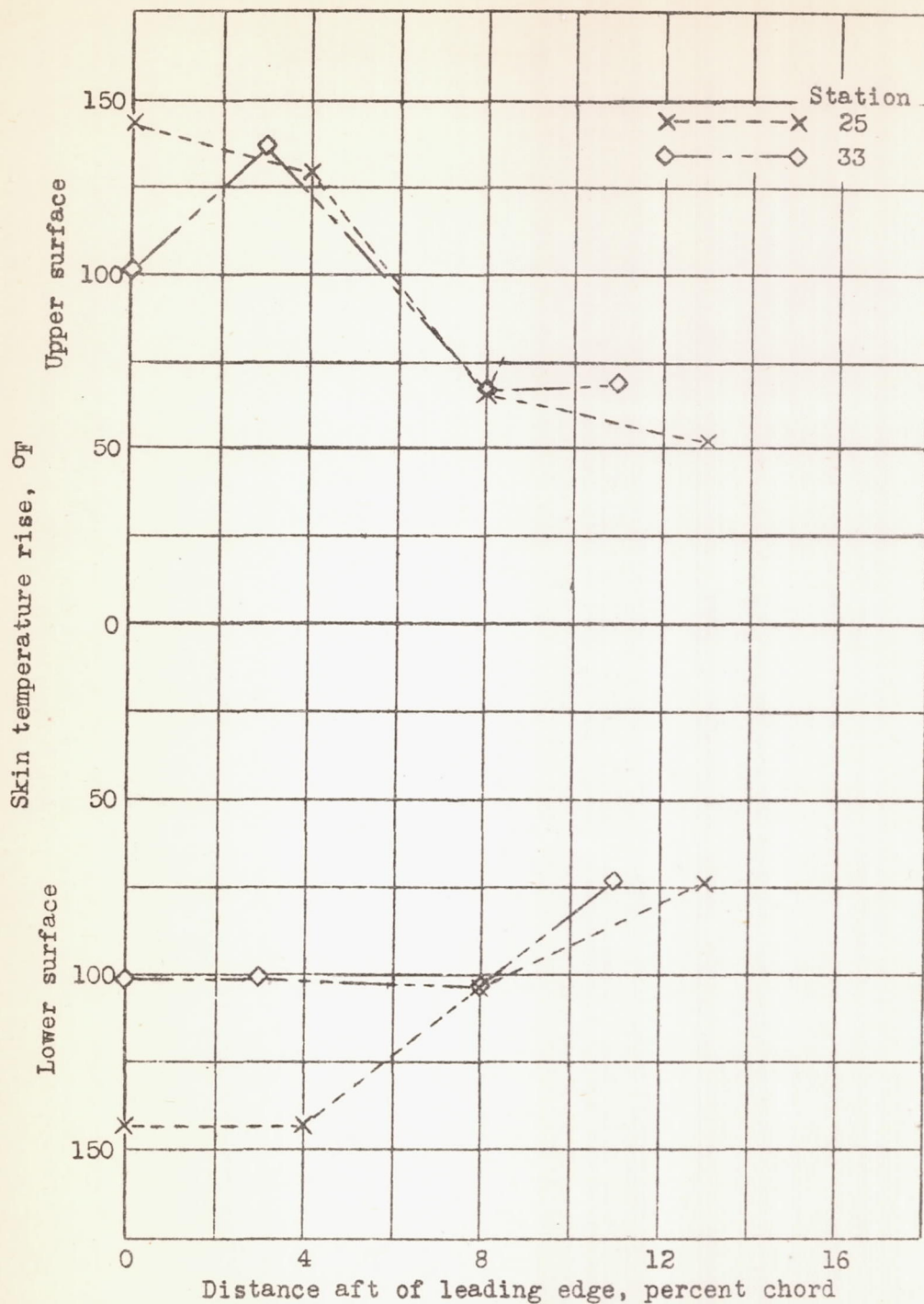


Figure 9.- Chordwise distribution of the skin temperature rise above ambient air temperature of the wing outer panel leading edge at stations 25 and 33. Test number 1; ambient air temperature, 3° F.

A-23



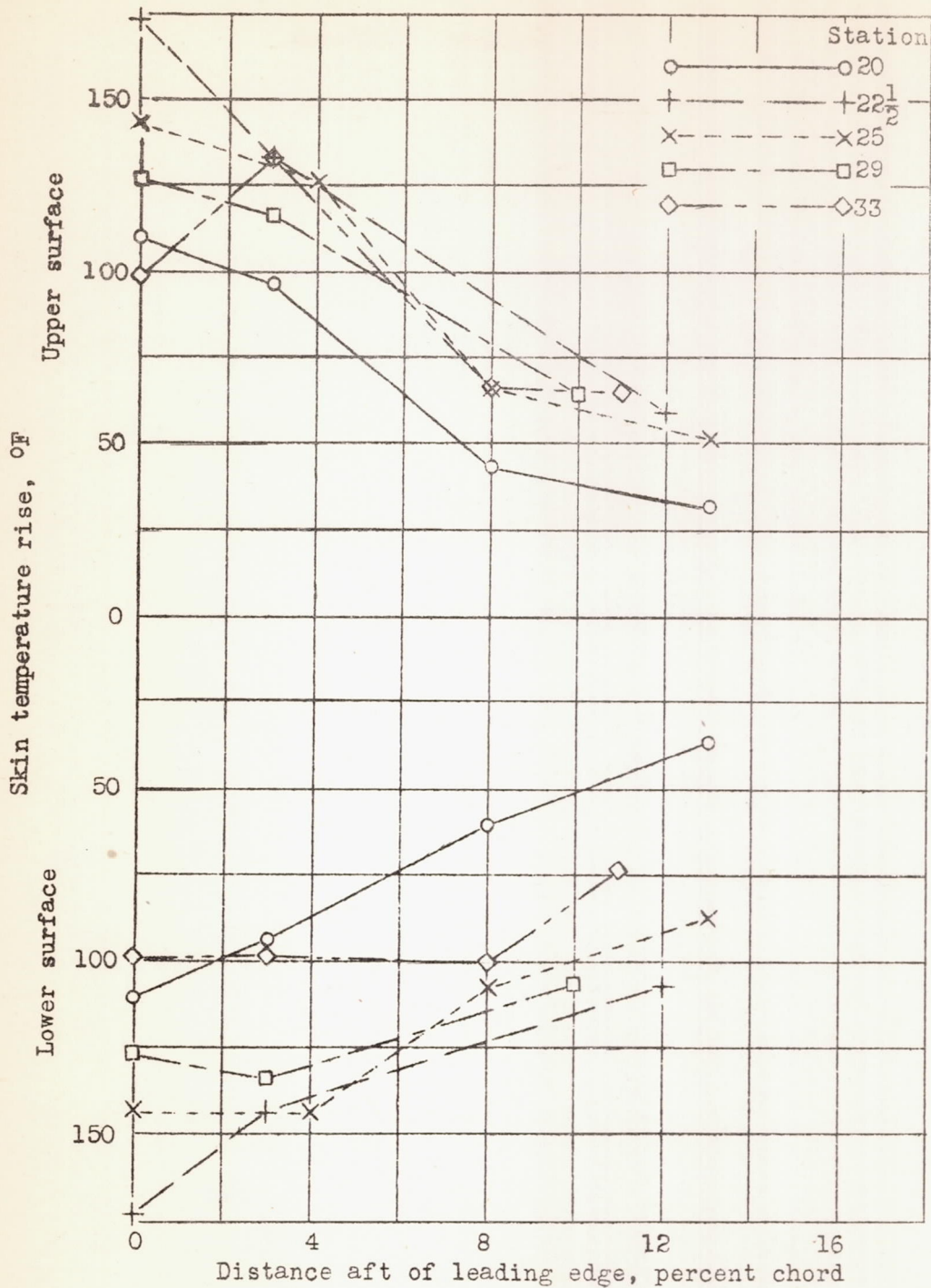


Figure 10.- Chordwise distribution of the skin temperature rise above ambient air temperature of the wing outer panel leading edge at stations 20, 22 1/2, 25, 29 and 33. Test number 2; ambient air temperature, 4° F.

A-23

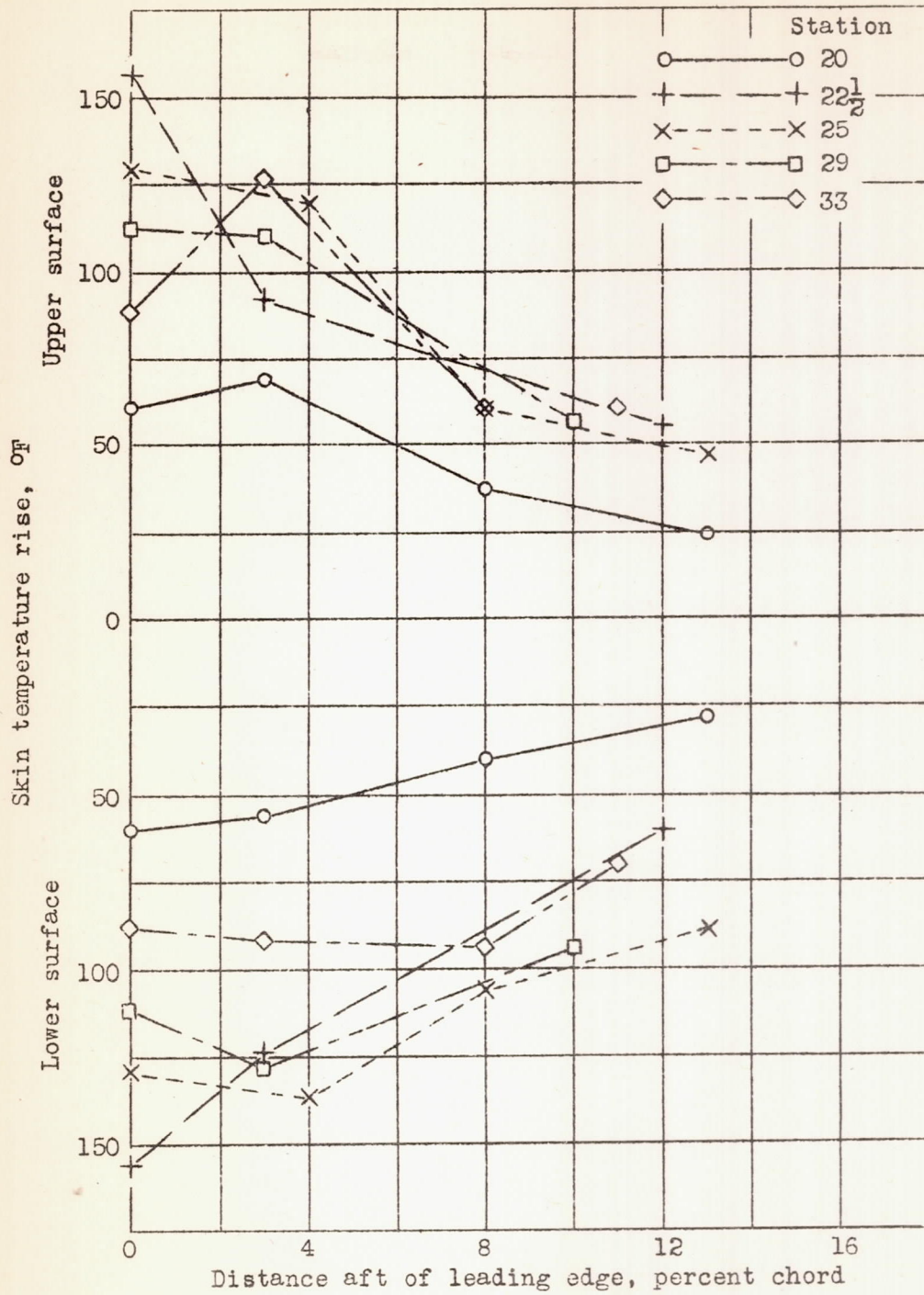


Figure 11.- Chordwise distribution of the skin temperature rise above ambient air temperature of the wing outer panel leading edge at stations 20, 22 1/2, 25, 29 and 33. Test number 3; ambient air temperature, 26° F.

A-23

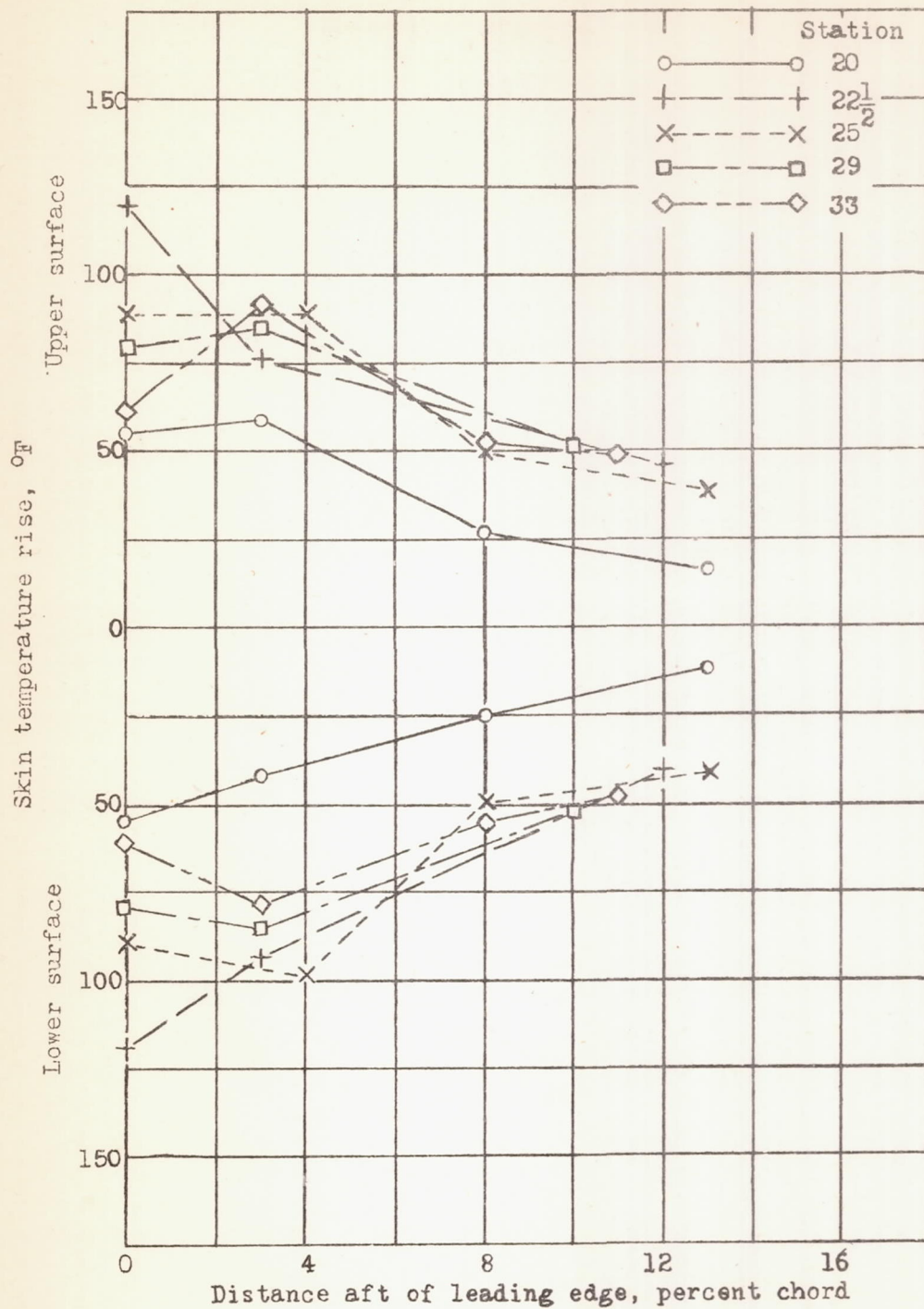


Figure 12.- Chordwise distribution of the skin temperature rise above ambient air temperature of the wing outer panel leading edge at stations 20, 22 1/2, 25, 29 and 33. Test number 4; ambient air temperature, 24° F.

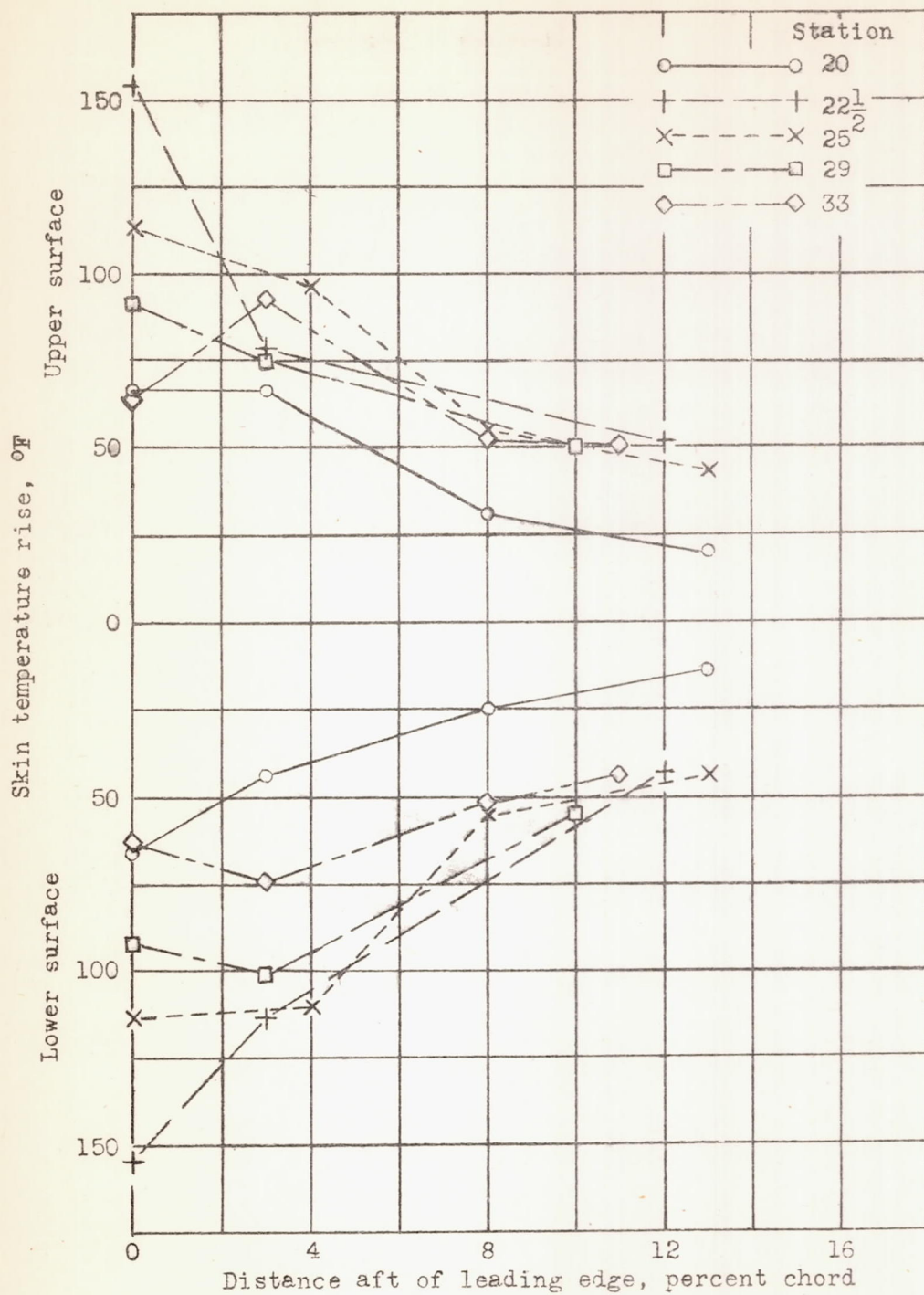


Figure 13.- Chordwise distribution of the skin temperature rise above ambient air temperature of the wing outer panel leading edge at stations 20, 22 1/2, 25, 29 and 33. Test number 5; ambient air temperature, 25° F.

A-23

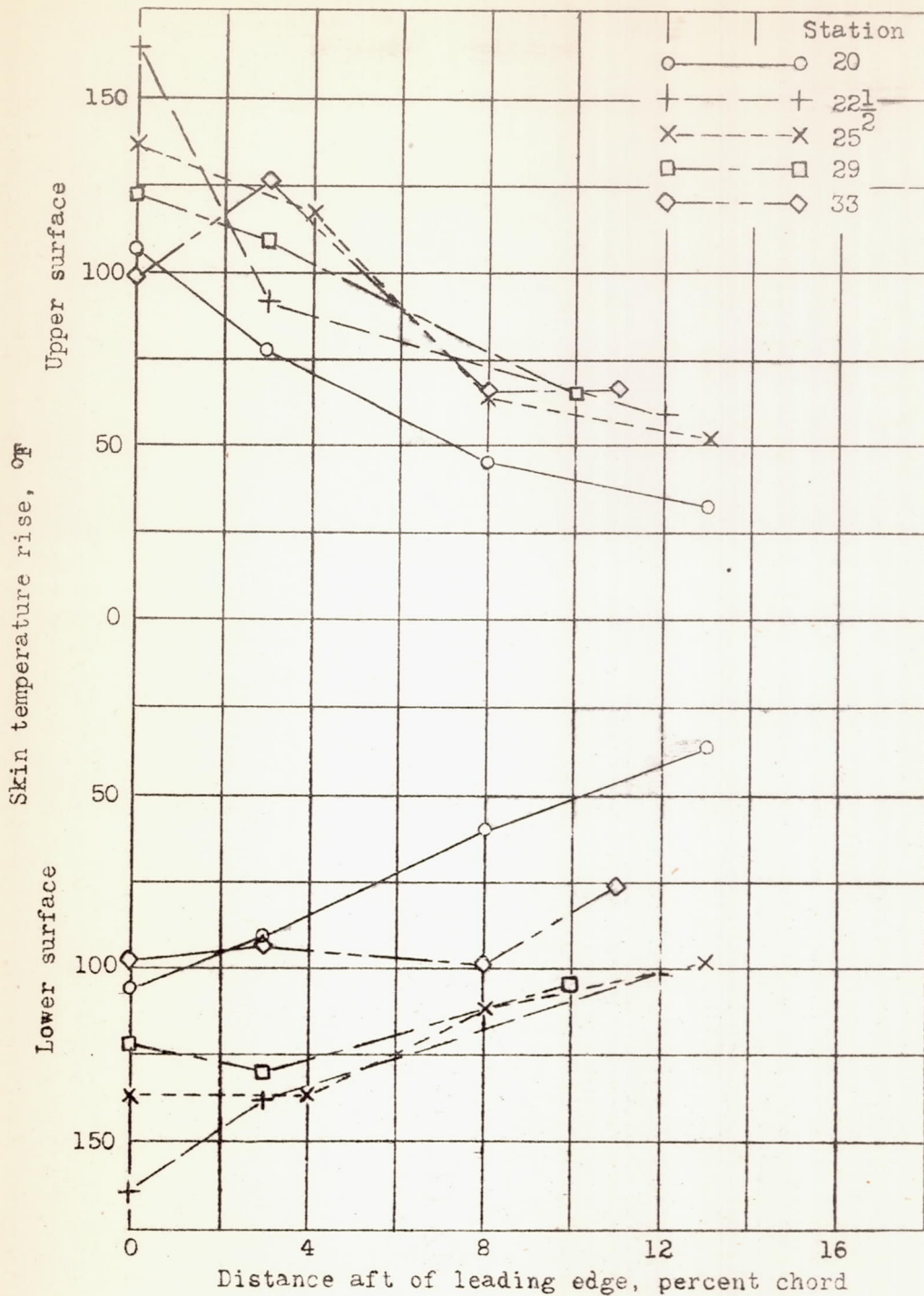


Figure 14.- Chordwise distribution of the skin temperature rise above ambient air temperature of the wing outer panel leading edge at stations 20, 22 1/2, 25, 29 and 33. Test number 6; ambient air temperature. 18° F.

A-23

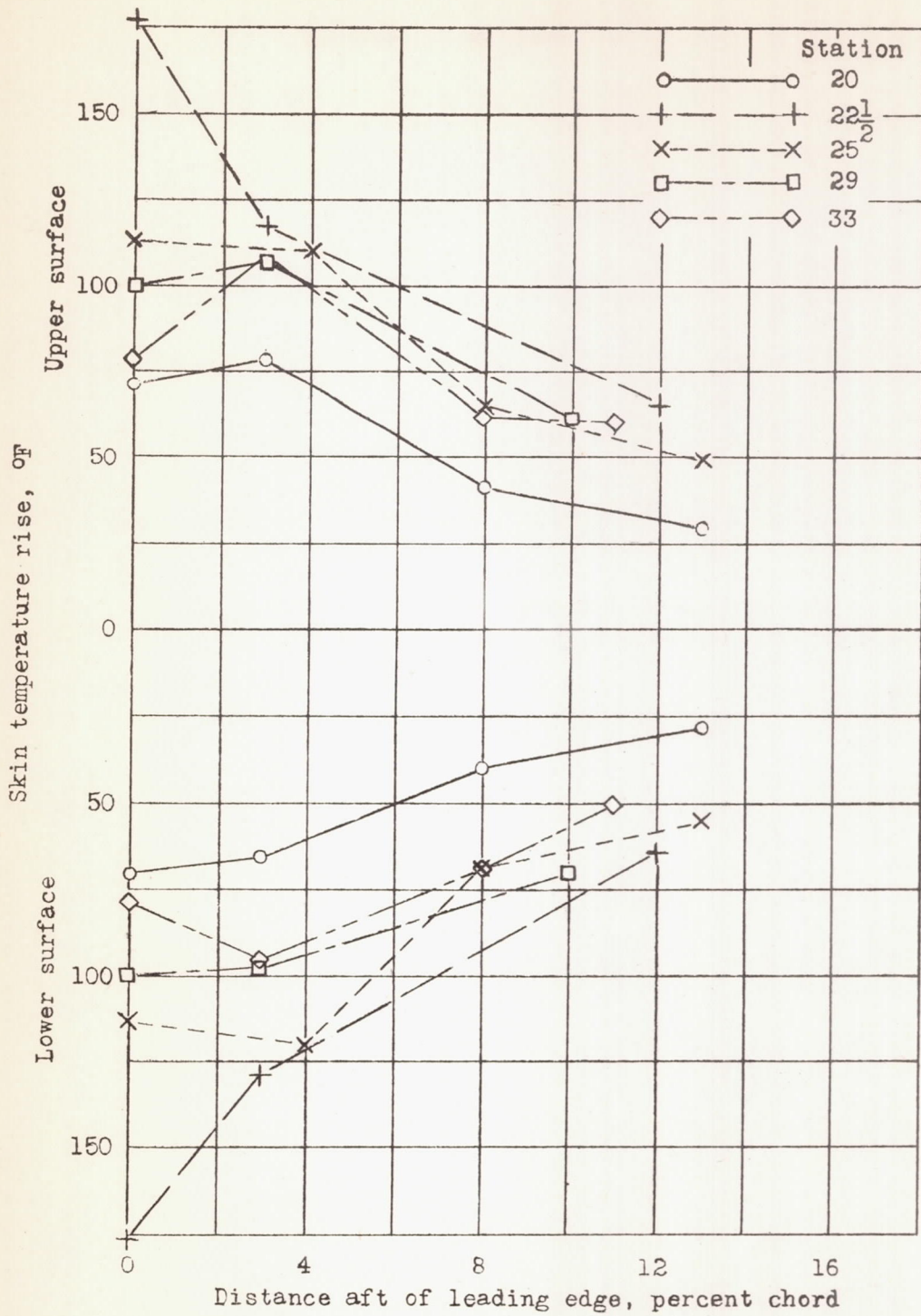


Figure 15.- Chordwise distribution of the skin temperature rise above ambient air temperature of the wing outer panel leading edge at stations 20, 22 1/2, 25, 29 and 33. Test number 7; ambient air temperature, 13° F.

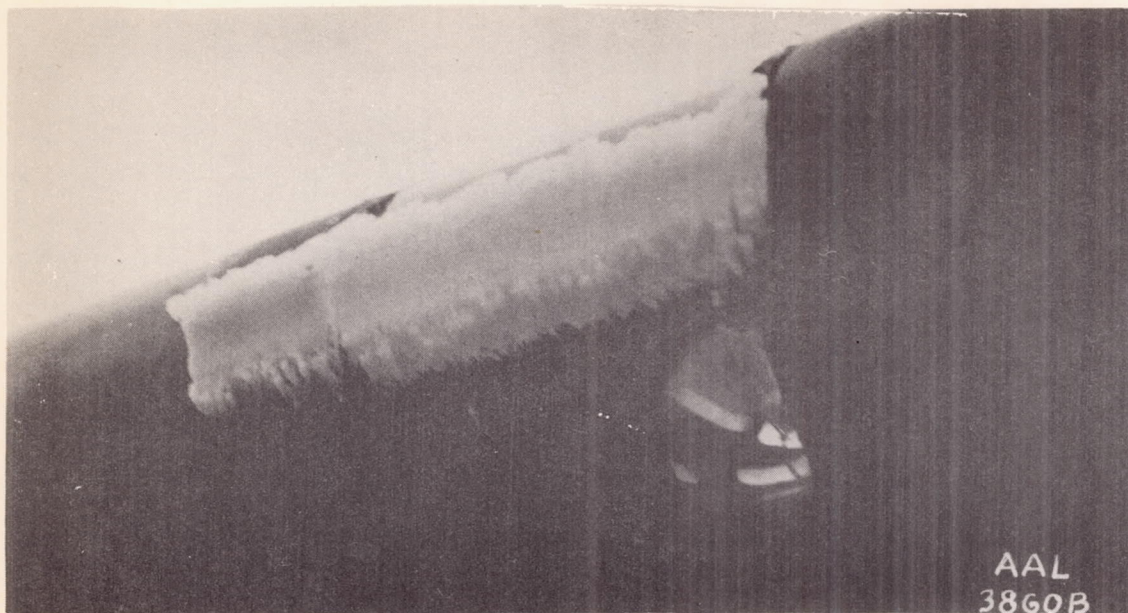


Figure 16.- Rime-ice formation on the right-hand landing-light cover and on the unheated leading edge at the wing splice. The photograph was taken after landing from test 7.

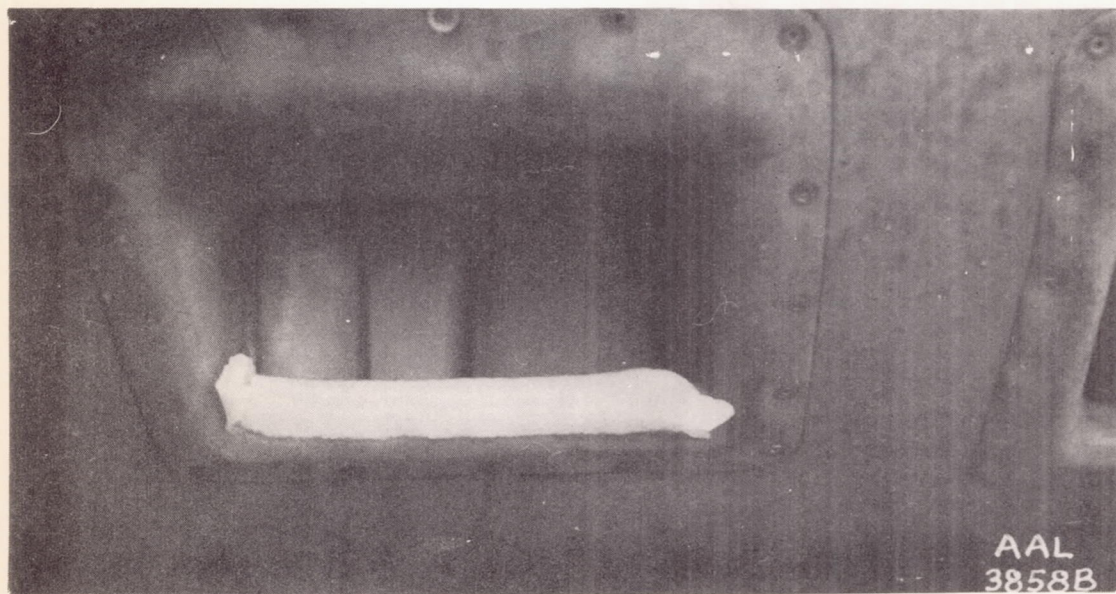


Figure 19.- Rime-ice formation on the lower lip and on the turning vanes in the duct of the intercooler air inlet located in the left wing leading edge outboard of nacelle 1, accumulated during test 7. (Photographed after landing.)

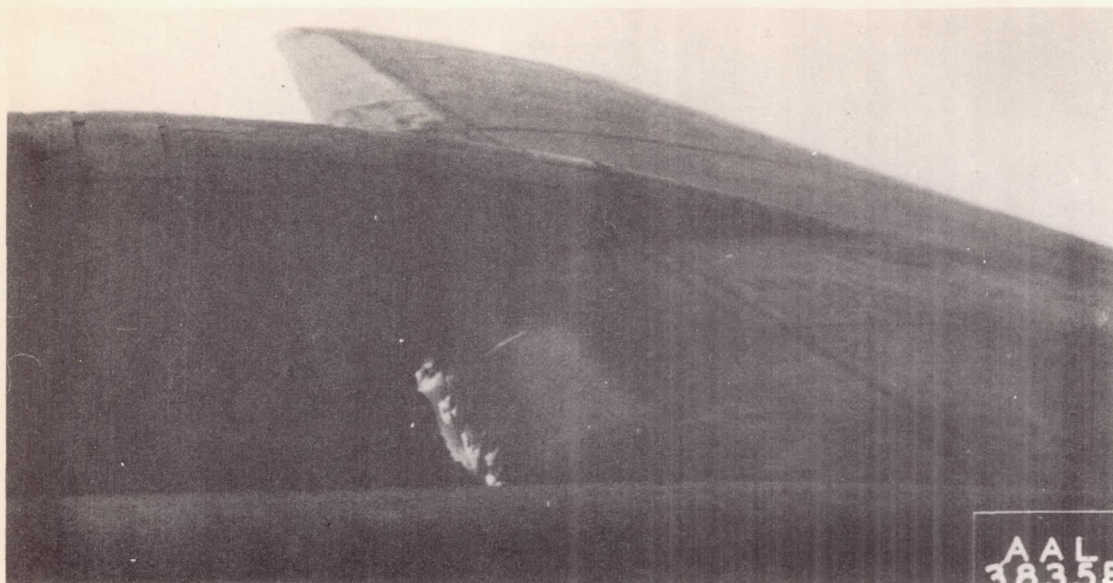


Figure 17.- Ice accumulation on the heated leading edge of the right-hand wing between nacelles 3 and 4 during test 7.

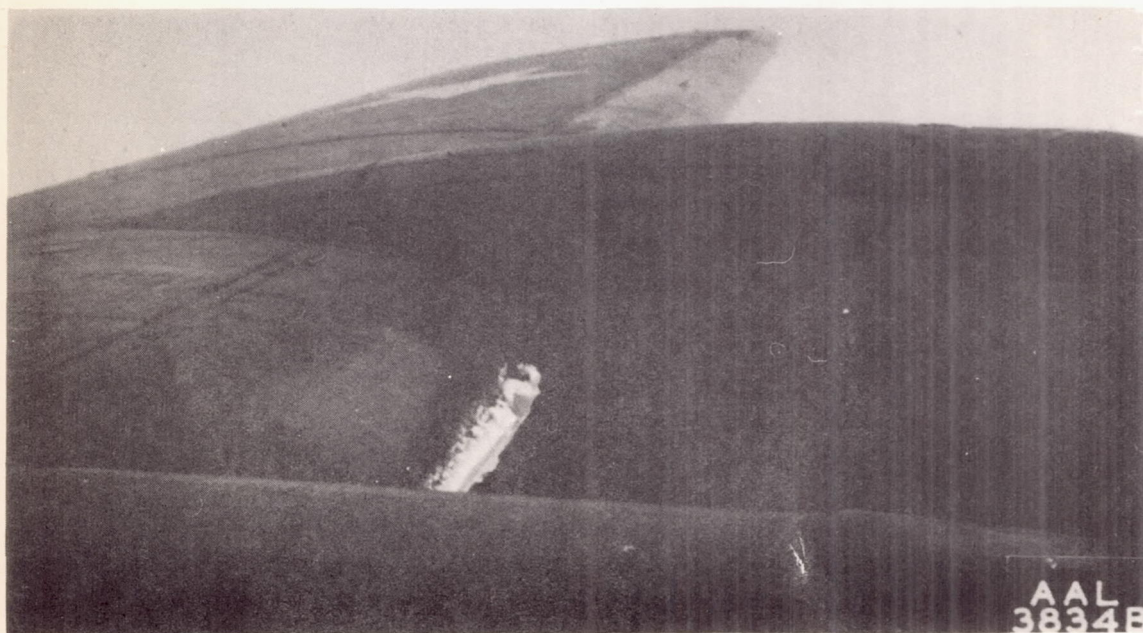


Figure 18.- Ice formation on the unheated leading edge of the left wing between nacelles 1 and 2, test 7.



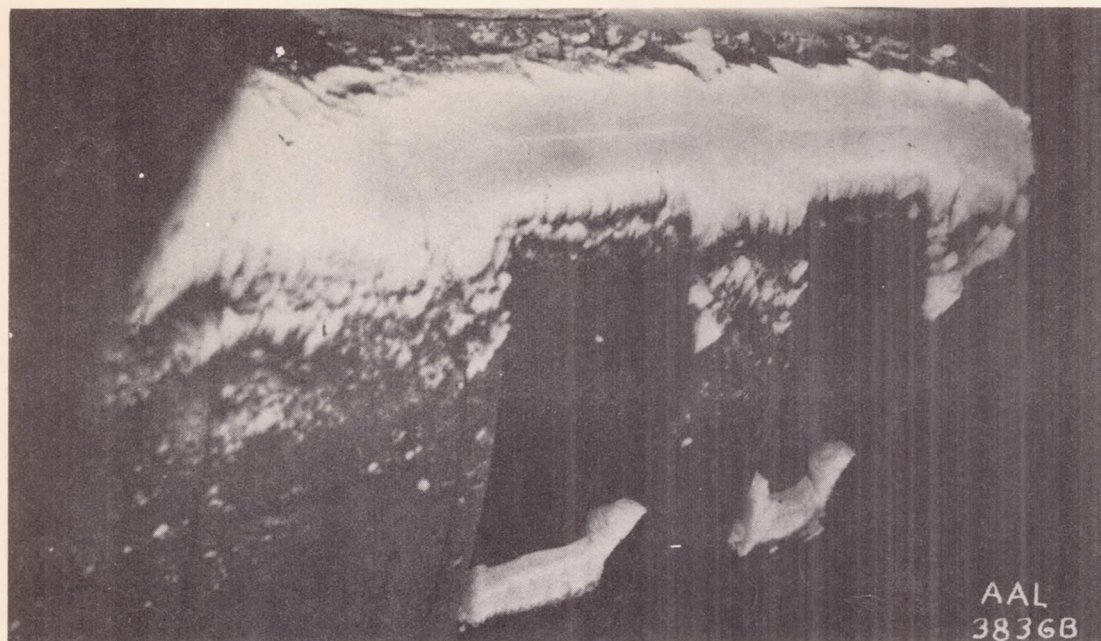


Figure 20.- Rime-ice formation on the unheated wing leading edge and carburetor and intercooler air inlets between the fuselage and the left inboard nacelle, accumulated during test 7. (Photograph taken after landing.)

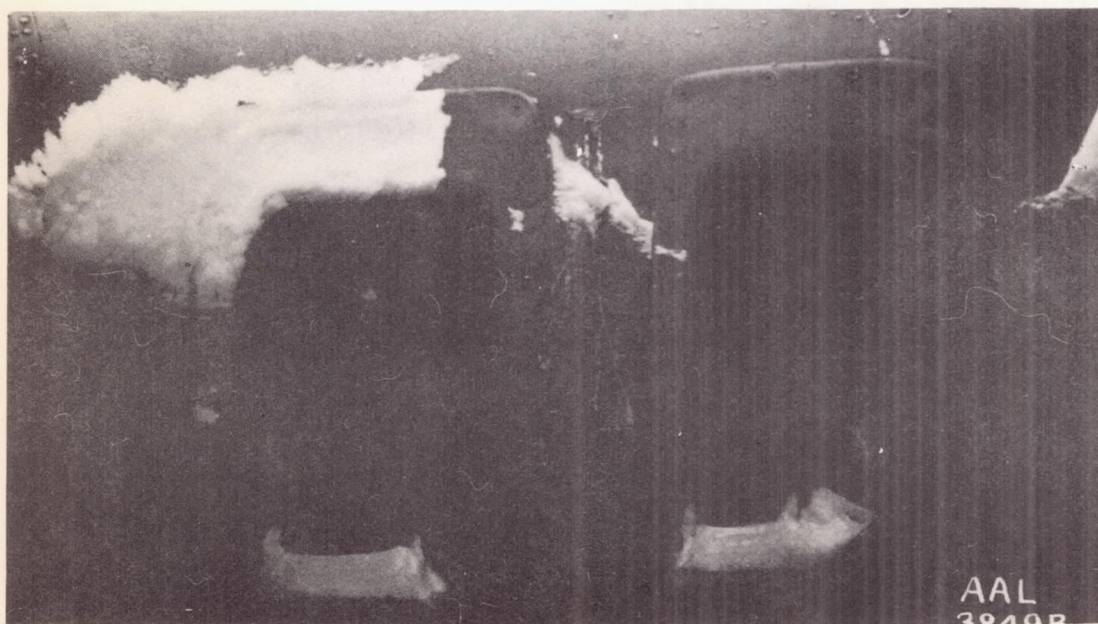


Figure 21.- Rime-ice accumulations around the carburetor and intercooler air inlets in the unheated wing leading edge between the fuselage and the right inboard nacelle during test 7. (Photograph taken after landing.)

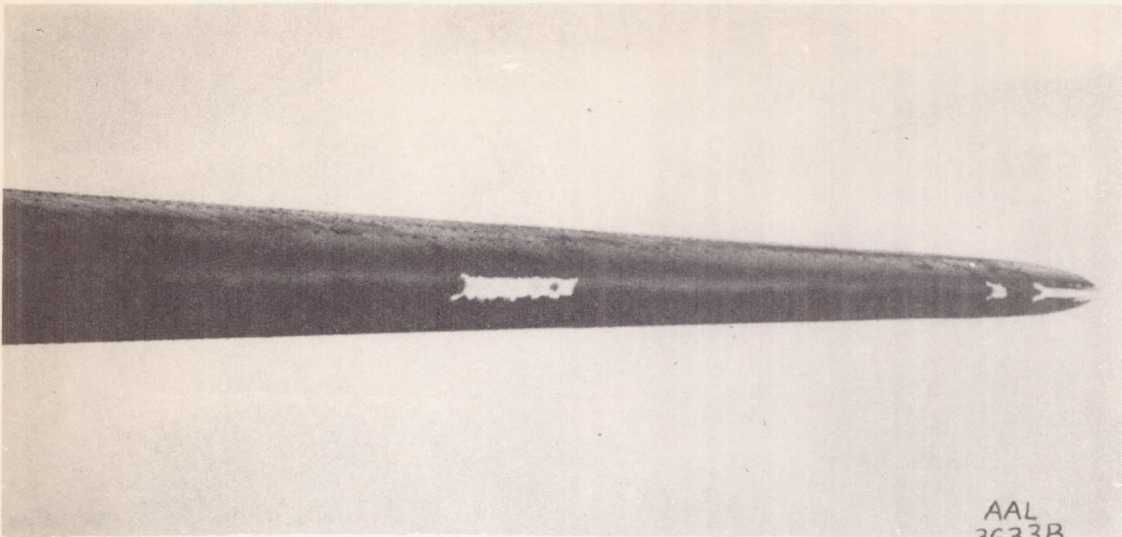


Figure 22.- Ice accumulations on the leading edge of the left horizontal stabilizer during flight of February 23, 1943.

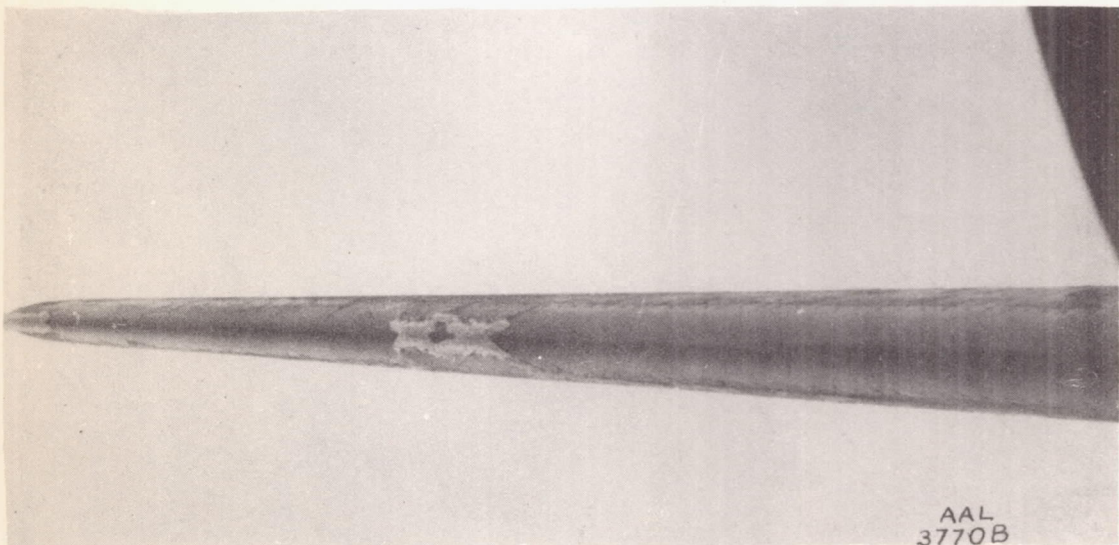


Figure 23.- Glaze-ice accumulation on leading edge of the right horizontal stabilizer at the tip, at mid-span, and in scattered areas on the aft portion of the double skin during tests 4 and 5.

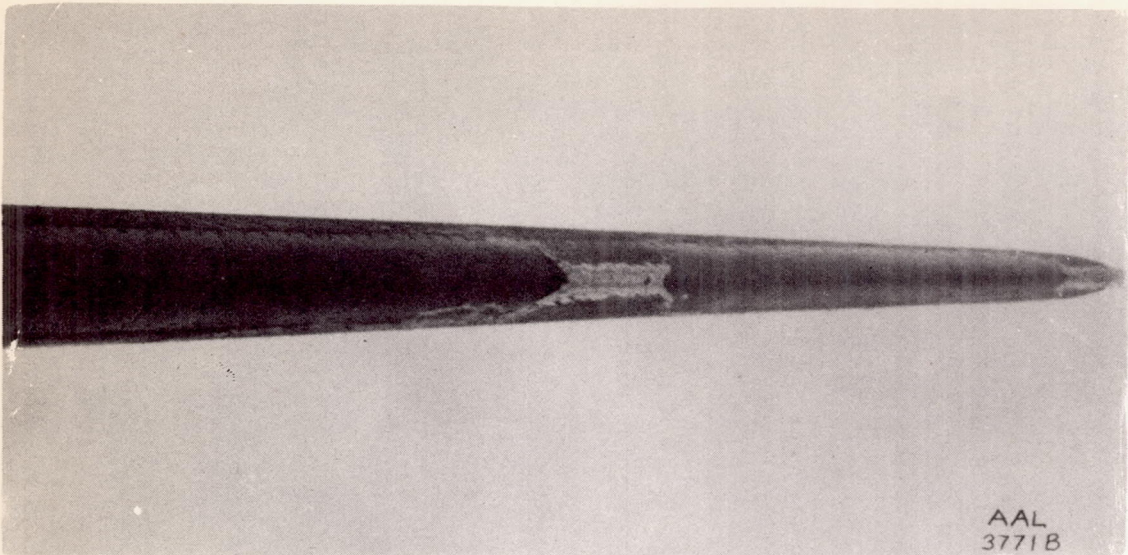


Figure 24.- Ice formation on the left horizontal stabilizer accumulated during tests 4 and 5.

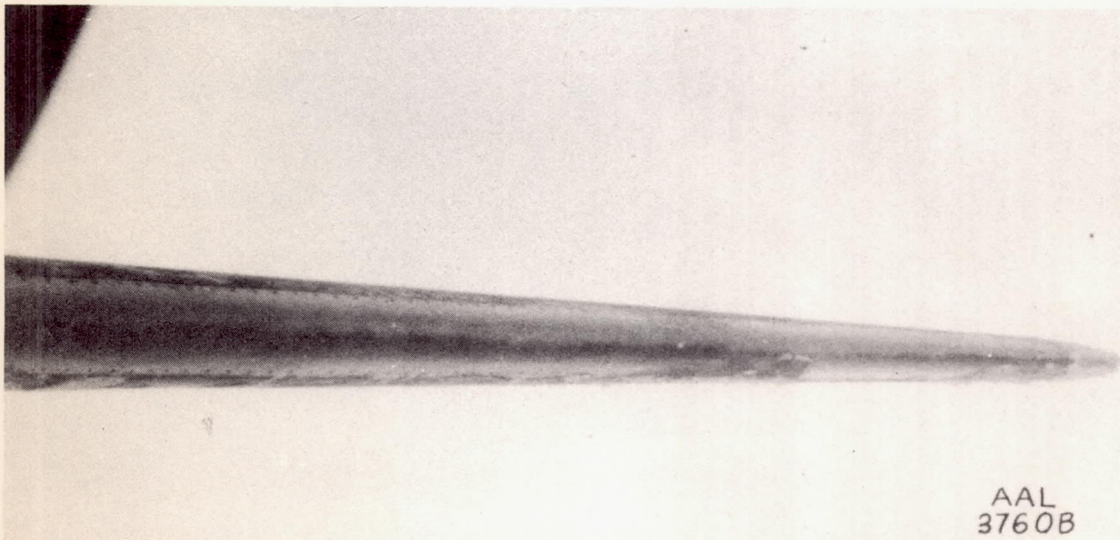


Figure 25.- Ice formation on the leading edge of the left horizontal stabilizer tip, on the aft portion of the double skin, and aft of the double skin on the upper and lower surfaces, accumulated during tests 4 and 5.

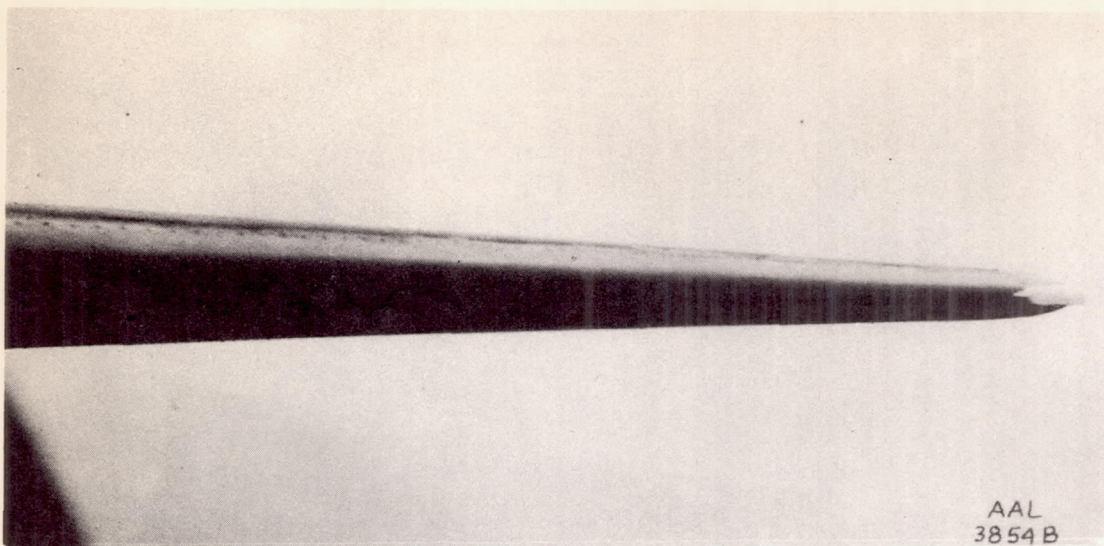


Figure 26.- Rime-ice accumulation on the left horizontal stabilizer during test 7.

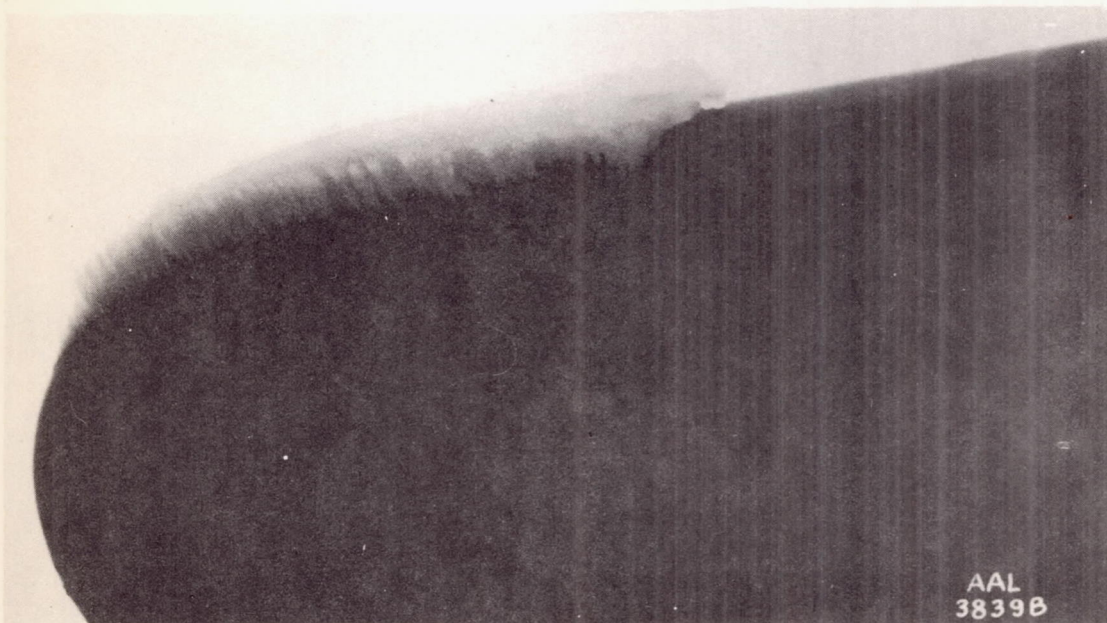


Figure 27.- Rime-ice accumulation on the right horizontal stabilizer tip during test 7. (Photograph taken after landing.)

A-23

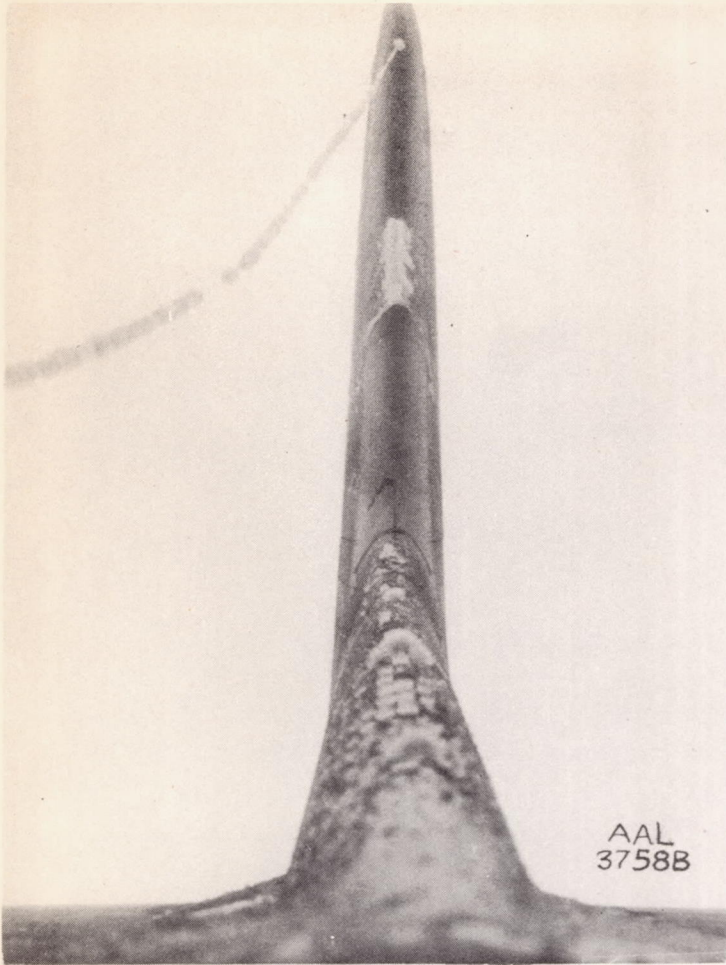


Figure 28.- The vertical stabilizer showing ice accumulation on the heated leading edge in the region of the dorsal and fin joint, and on the unheated forward portion of the dorsal during tests 4 and 5.

Figure 29.- The vertical stabilizer showing the accumulation of ice on the leading edge of the dorsal forward of the heated double skin, on the leading edge at the junction of the dorsal and fin, at the fin tip, and aft of the leading edge during tests 4 and 5.



A-23

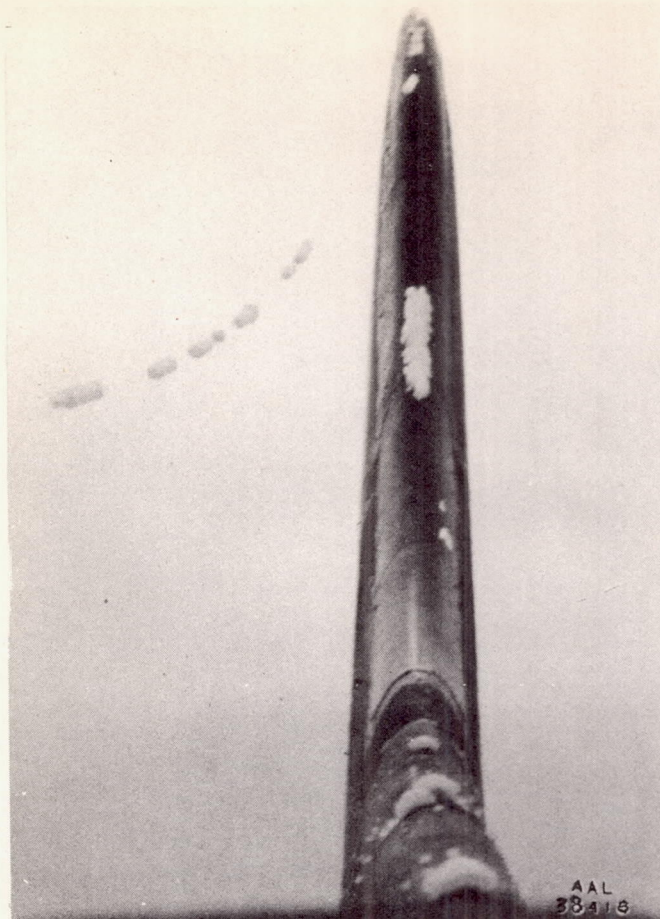


Figure 30.- Rime-ice formation on the heated leading edge of the vertical stabilizer at the junction of the dorsal and fin, at the tip of the fin, and on the running lights on the forward portion of the dorsal during test 7.



Figure 35.- Rime-ice formation on the forward side of the upper gun turret accumulated during test 7. (Photograph taken after landing.)

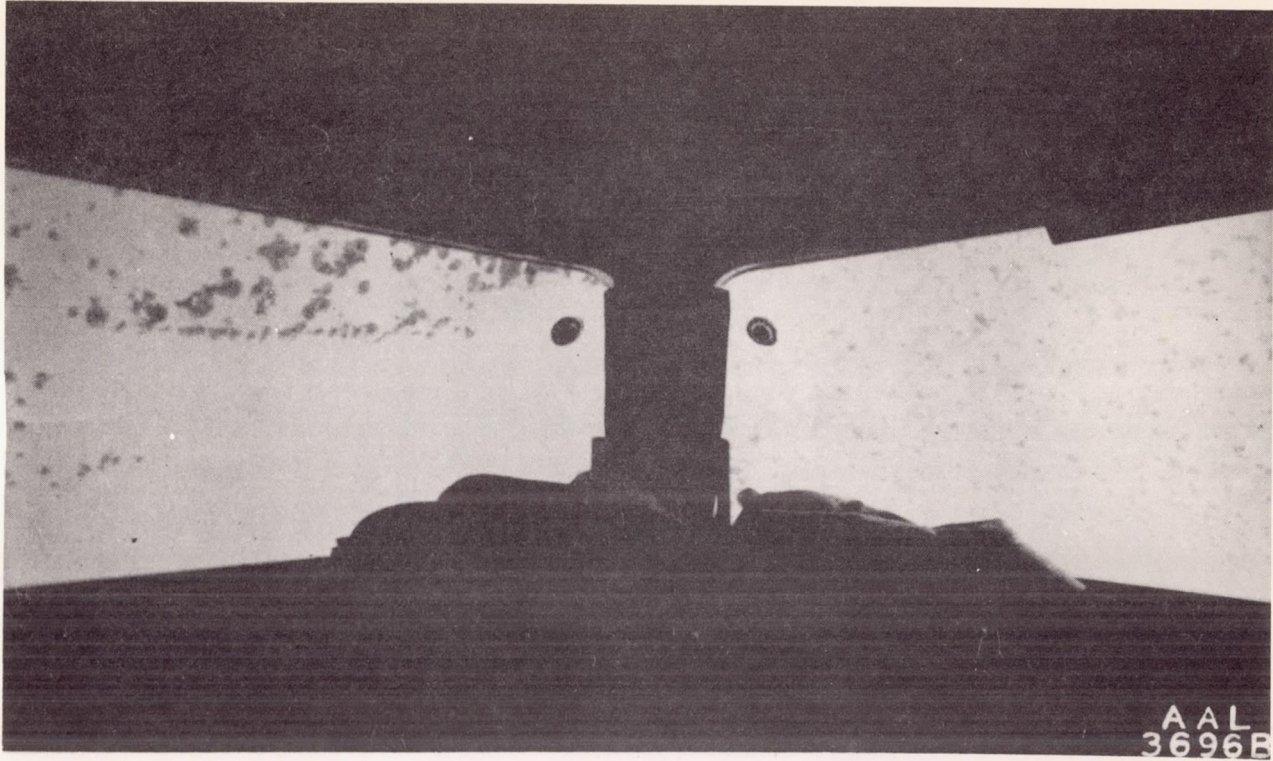


Figure 31.- Icing of pilot's (left) and copilot's (right) windshields during flight of February 23, 1943. The photograph shows the partial protection afforded the heated pilot's windshield.

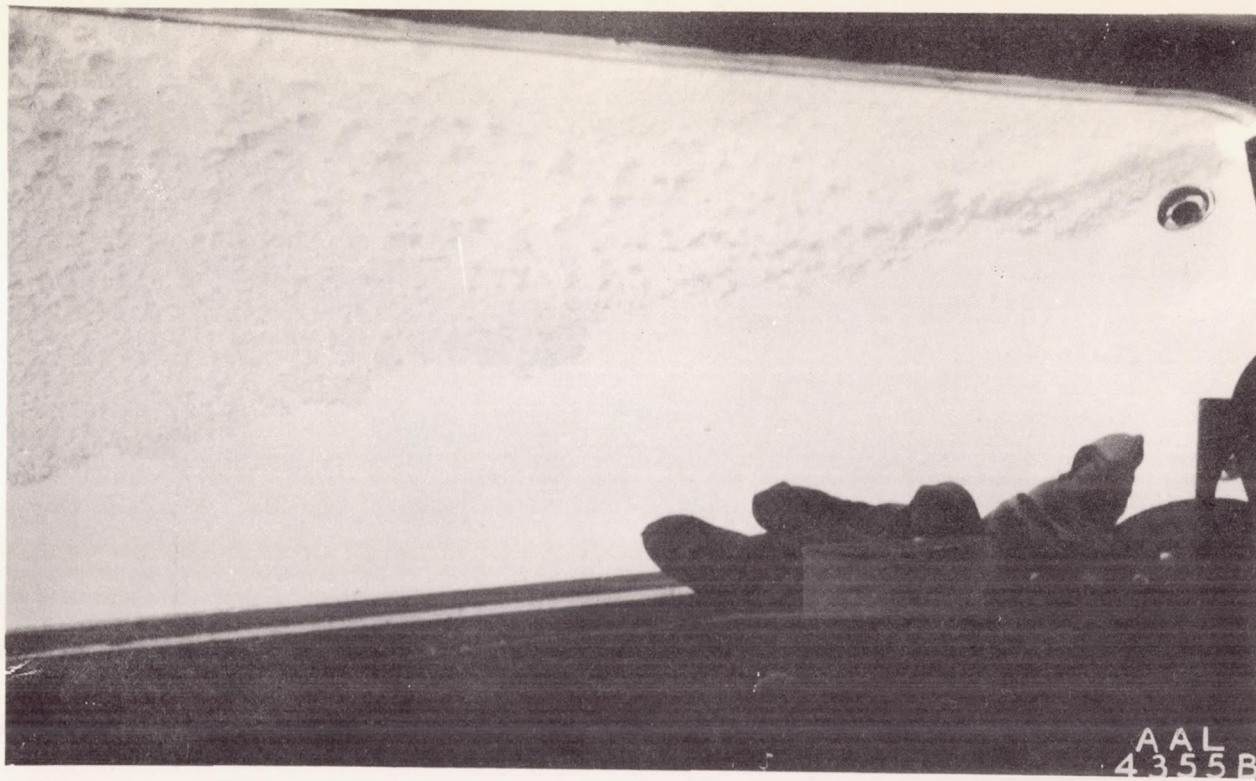


Figure 32.- Ice accumulation on the pilot's heated windshield during flight in icing, test 3.



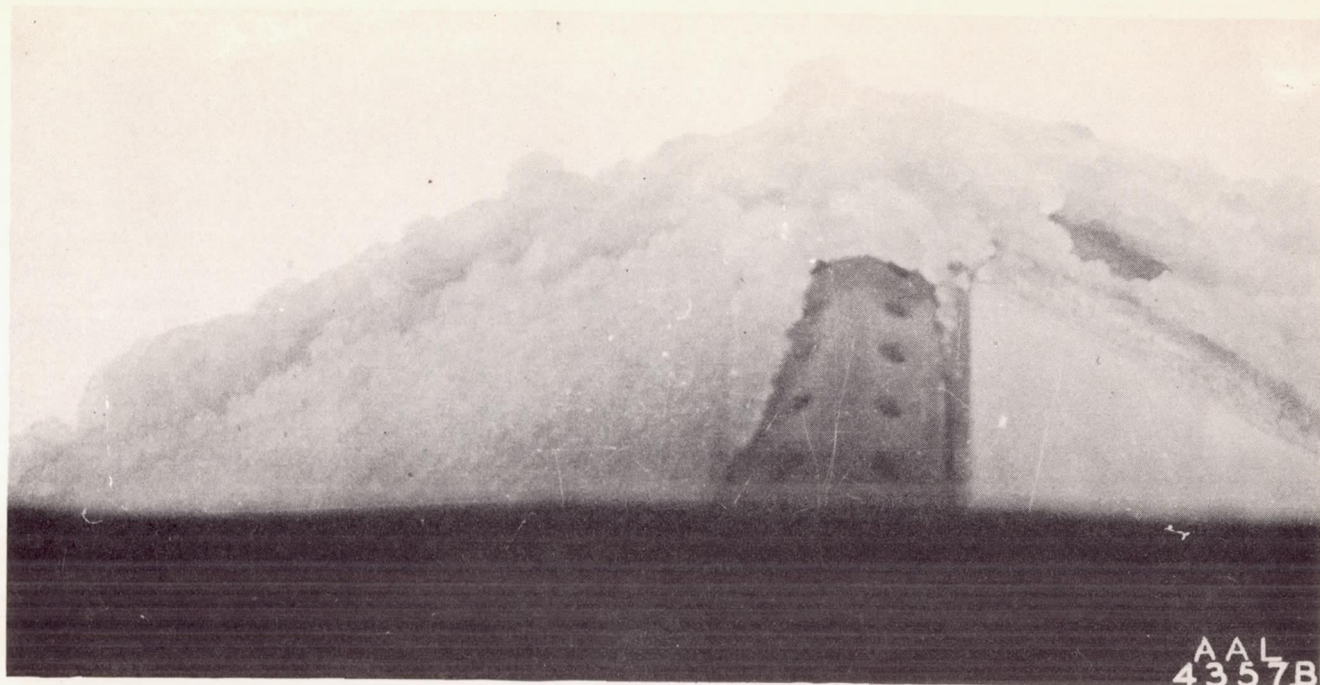


Figure 33.- Ice formation on the pilot's and copilot's windshield during test 3. The lower portion of the heated pilot's windshield (on the right) is clear of ice.

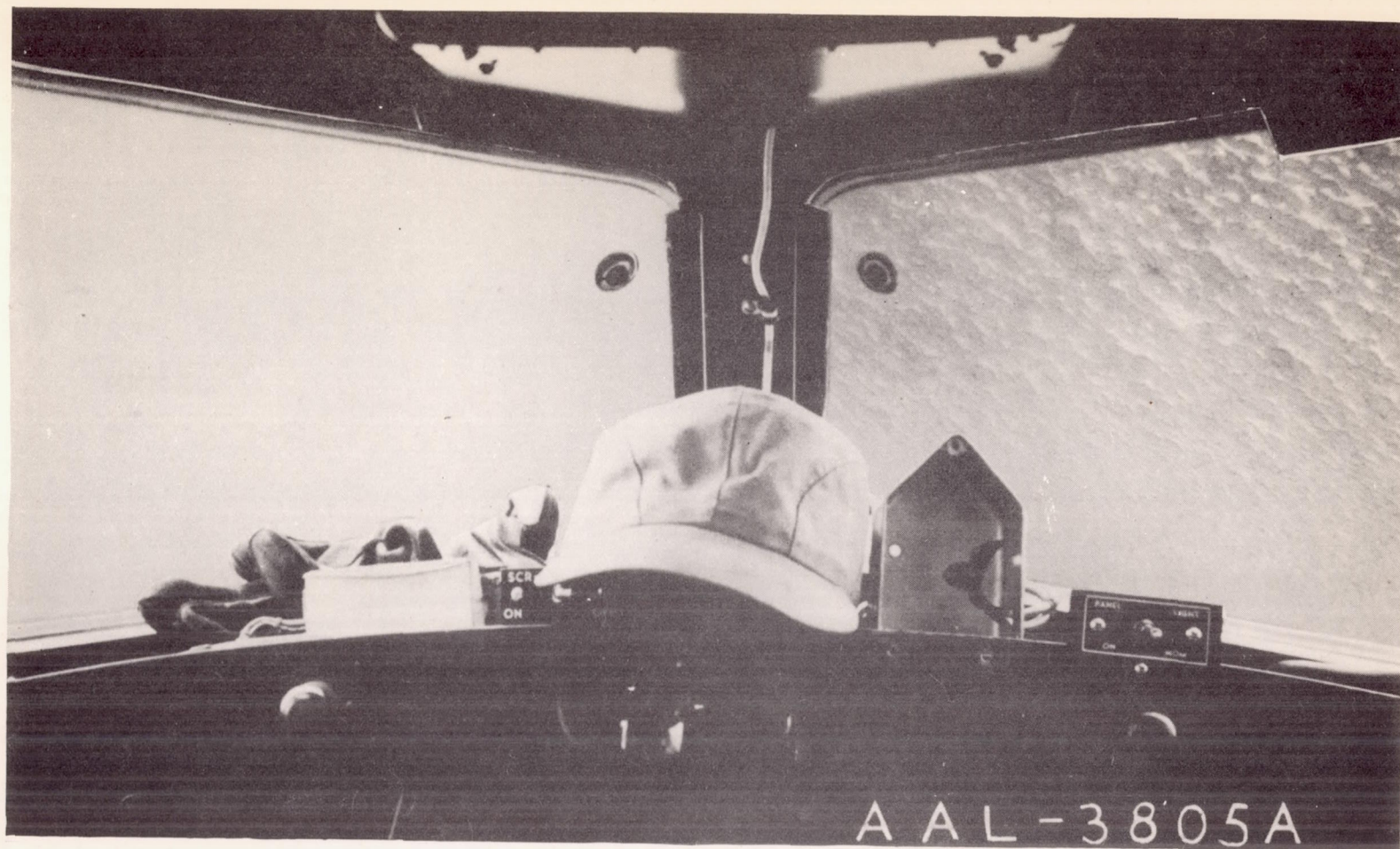


Figure 34.- The pilot's (left) and copilot's (right) windshields during tests 4 and 5, after leaving the icing region. The heated pilot's windshield is clear of ice.

A-23

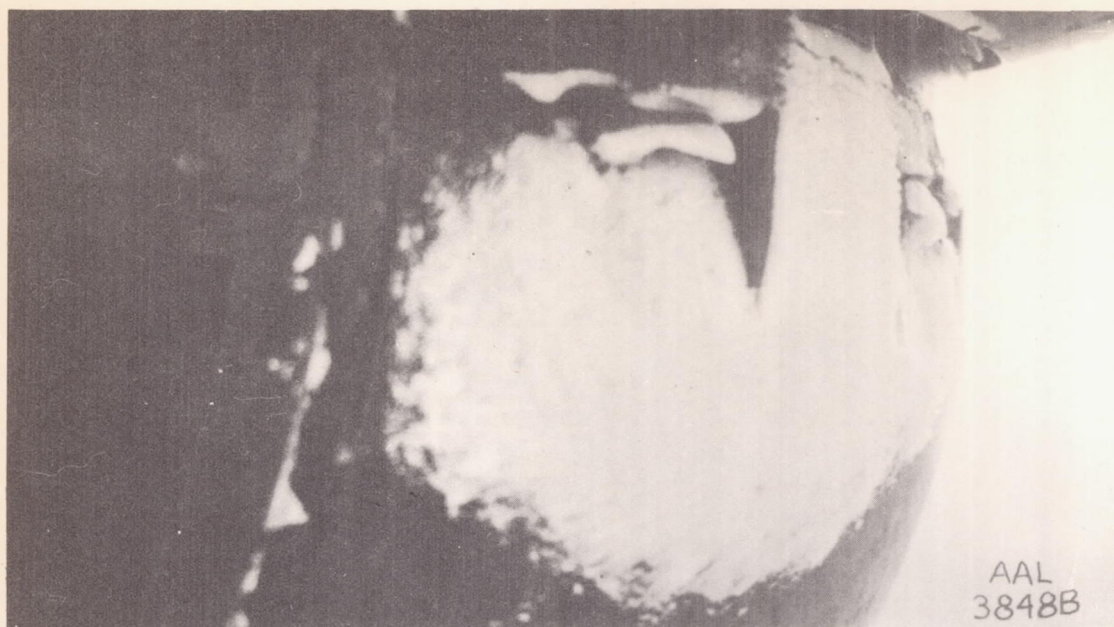


Figure 36.- Rime-ice accumulation on the forward edge of the ball turret during test 7. (Photograph taken after landing.)

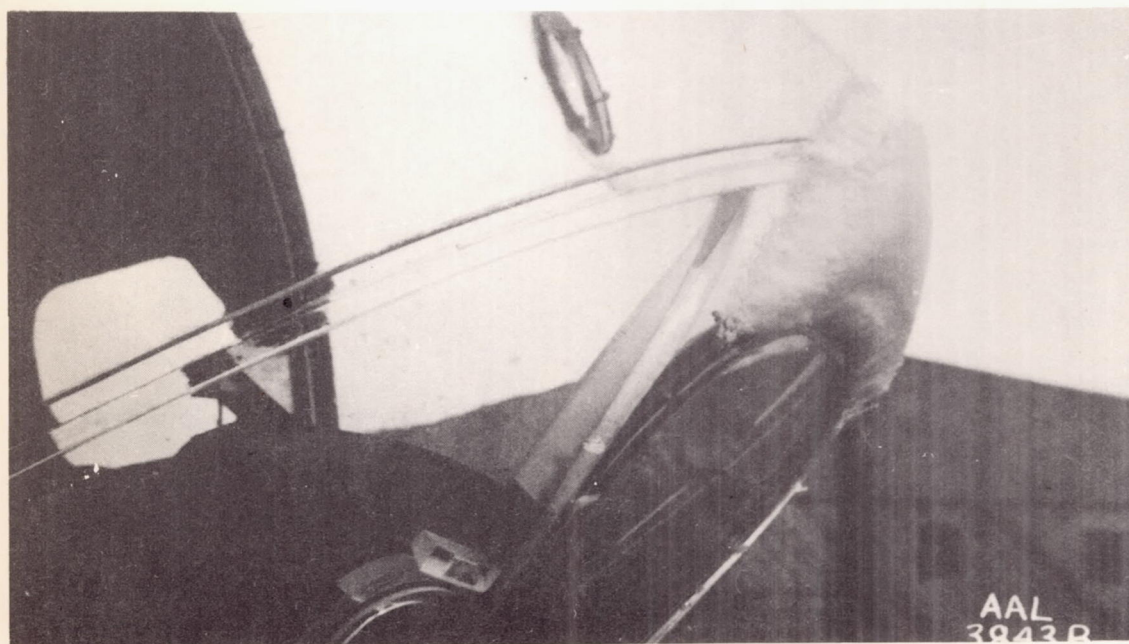


Figure 37.- Rime-ice accumulation on the front of the fuselage during test 7. (Photograph taken after landing.)

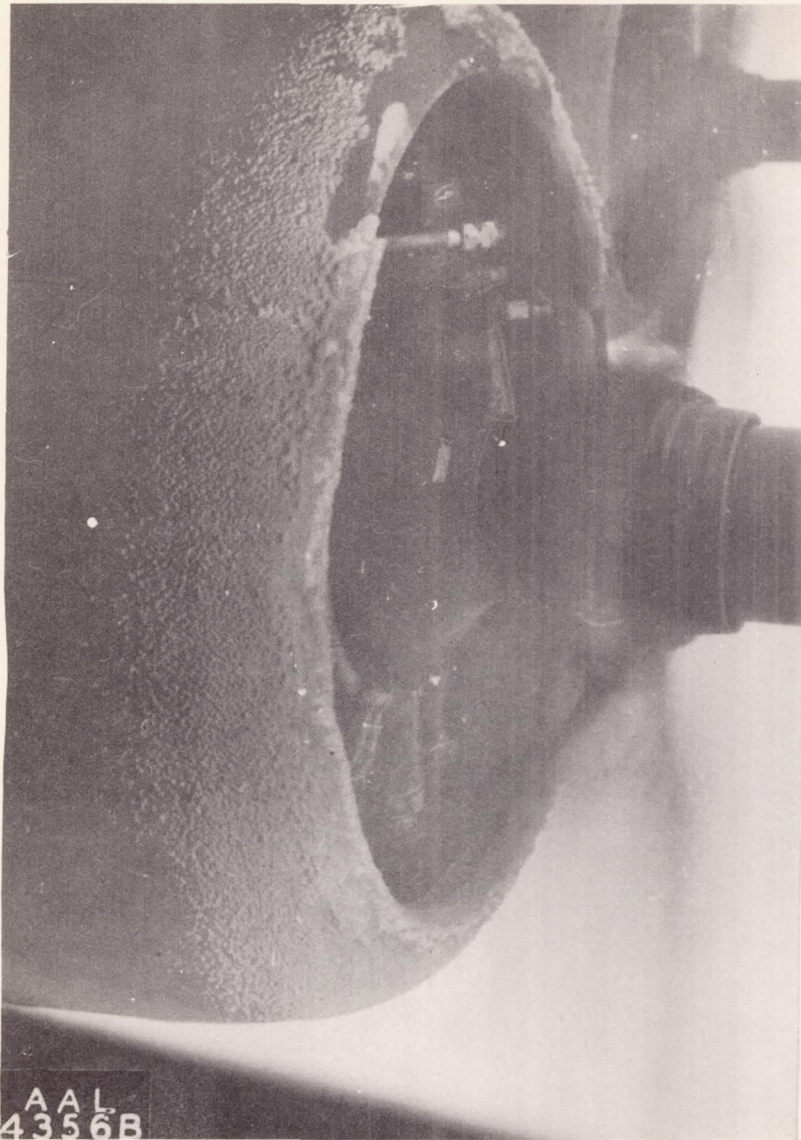


Figure 38.- Ice formation on the left inboard engine cowl accumulated during test 3.

A-23.

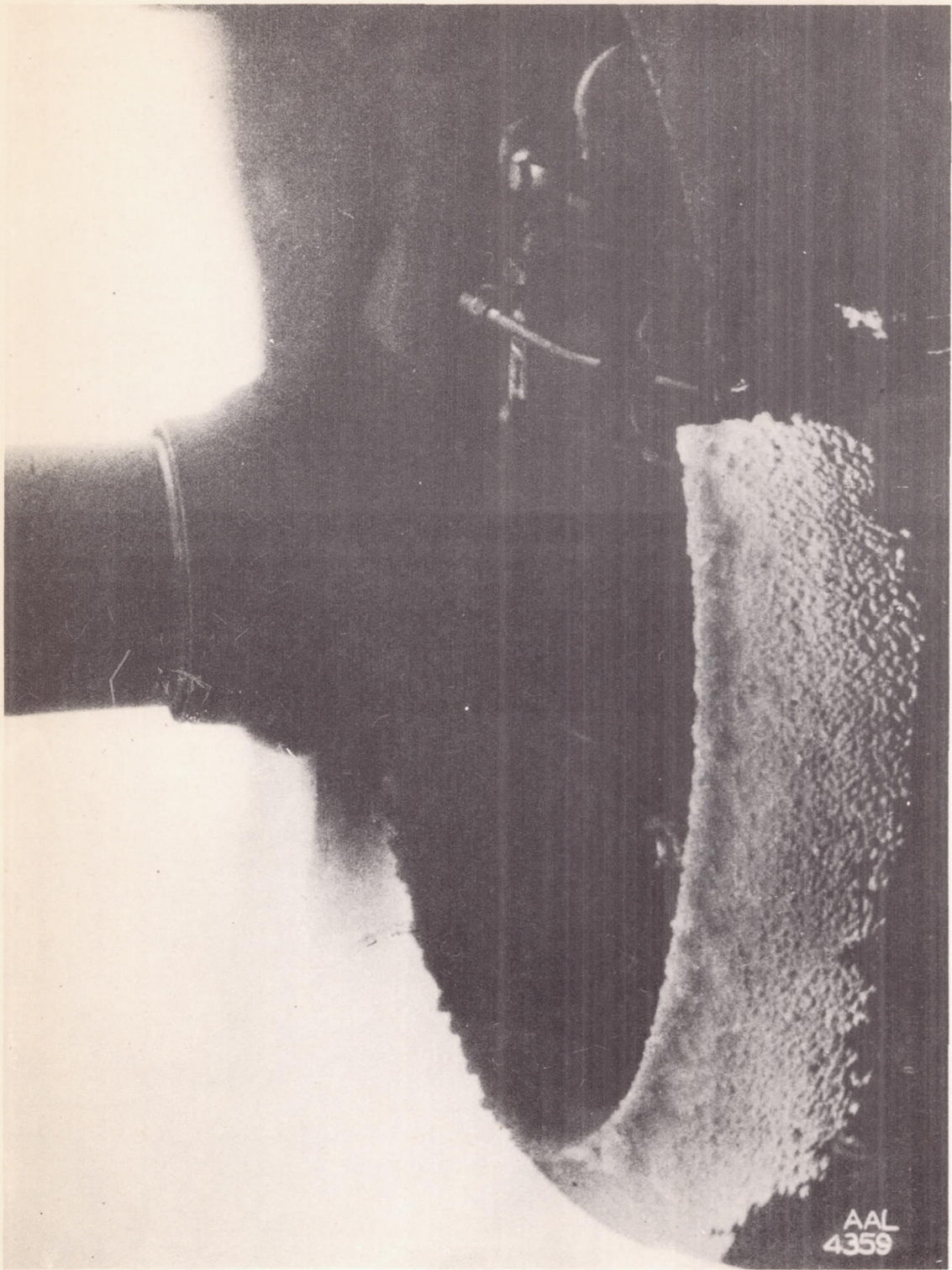


Figure 39.- Ice formation on the right inboard engine cowl accumulated during test 3.

A-23

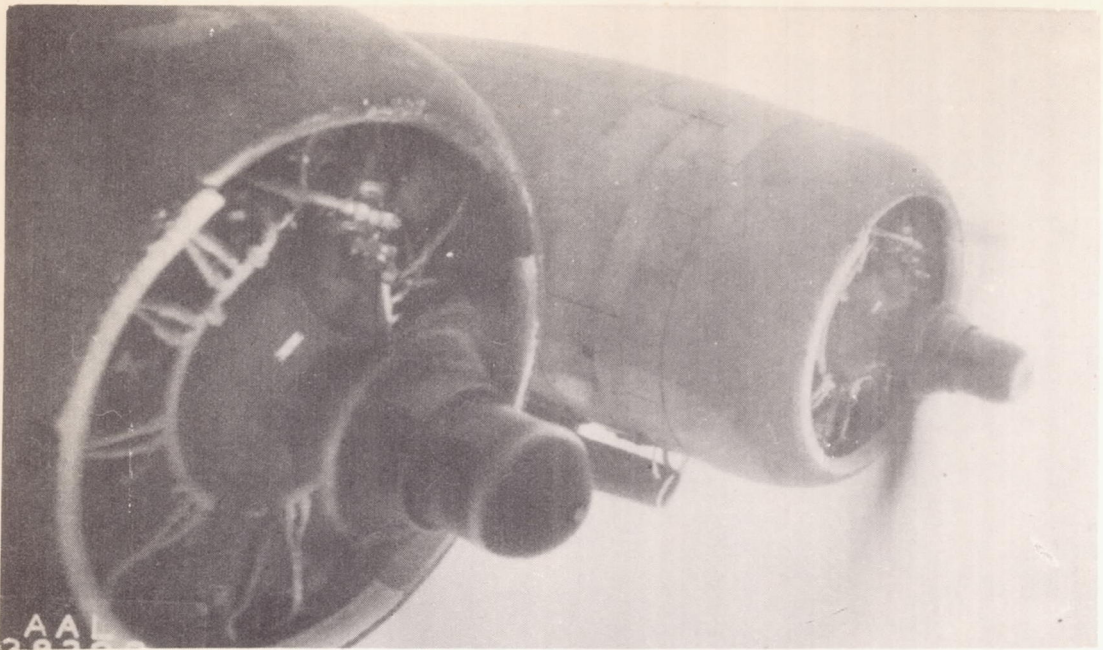


Figure 40.- The left engine nacelles showing ice accumulations on the leading edge of the cowls, and on the lip of the air inlet for the heat exchanger in the out-board nacelle (beneath the right nacelle) during test 7.

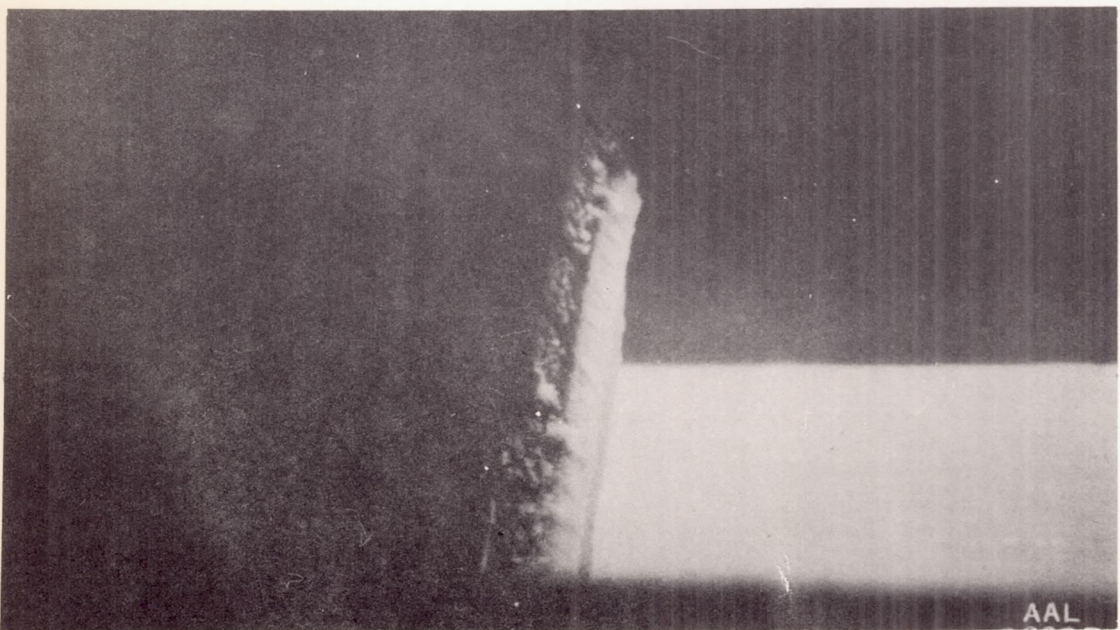


Figure 42.- Rime-ice accumulation on the unheated wing leading edge between the fuselage and the left in-board nacelle during test 7.

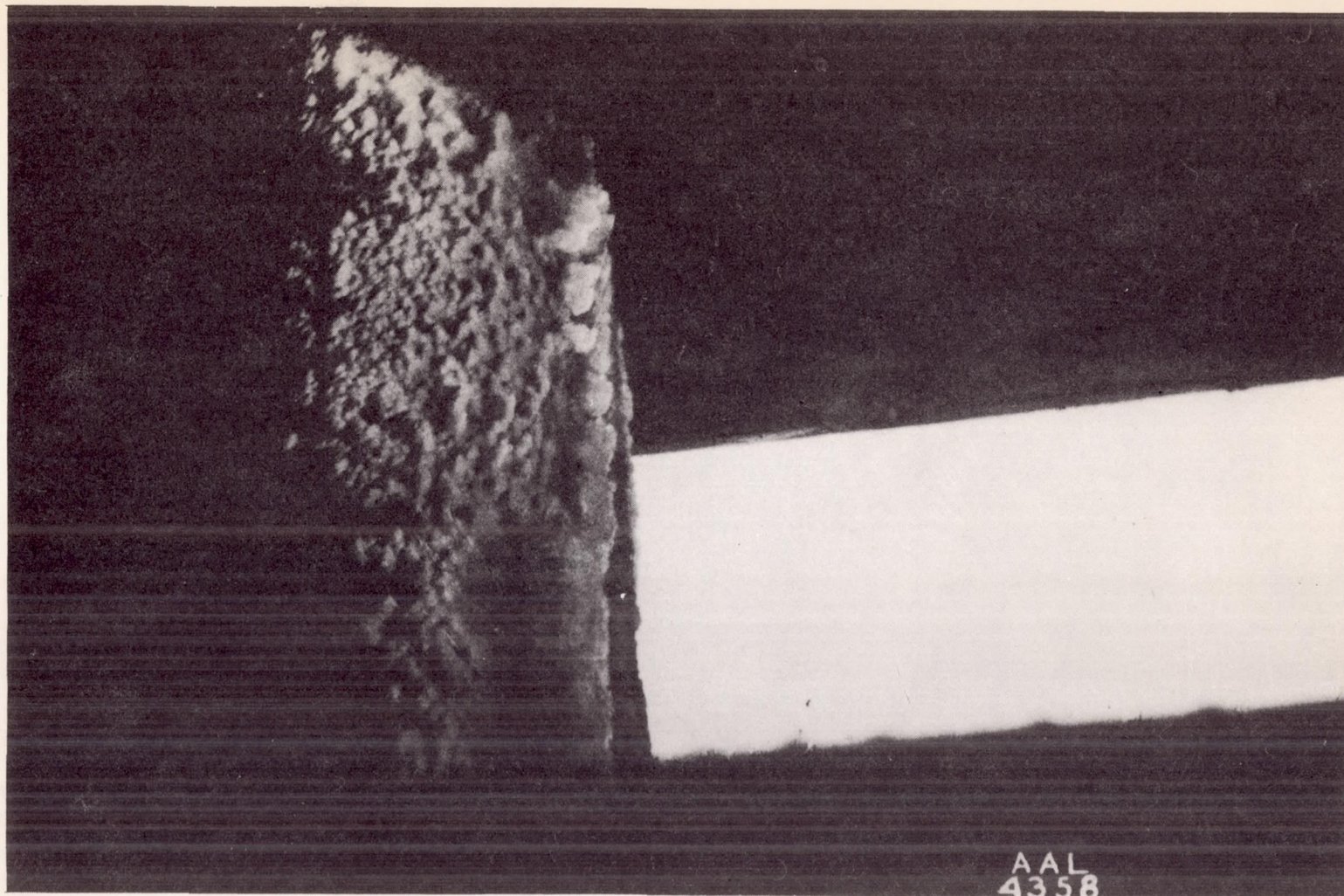


Figure 41.- The unheated wing leading edge, between the fuselage and the left in-board nacelle, showing ice formation accumulated during test 3.

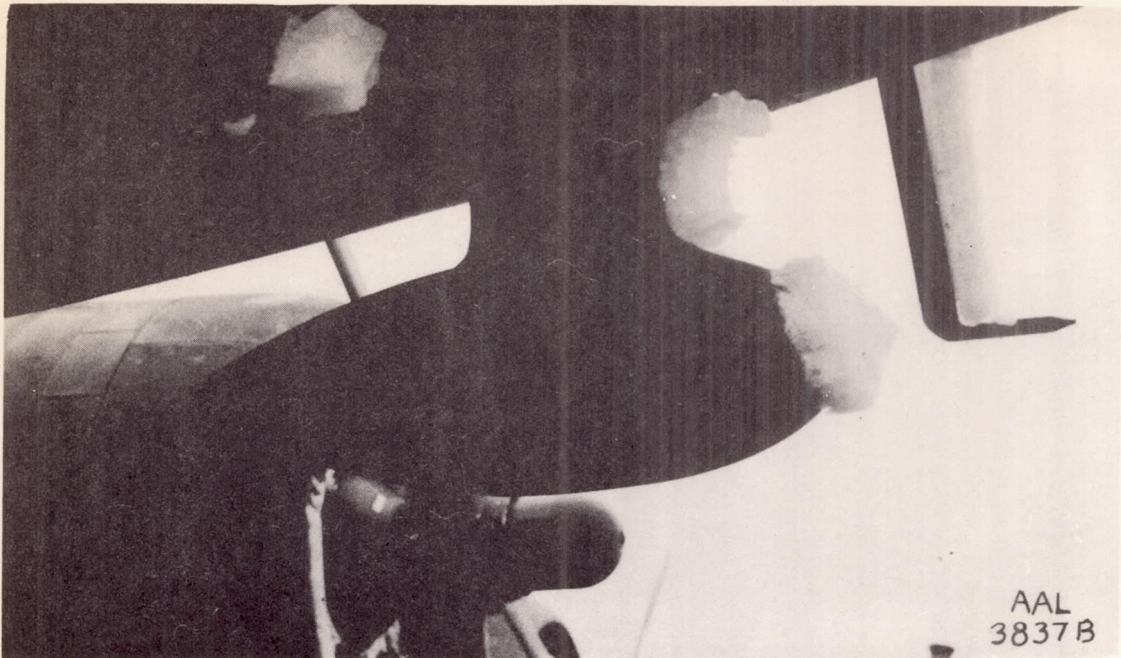


Figure 43.- Ice accumulations on the drift sight (left center in photograph), loop-antenna housing, and the left airspeed mast during test 7. (Photograph taken after landing.)

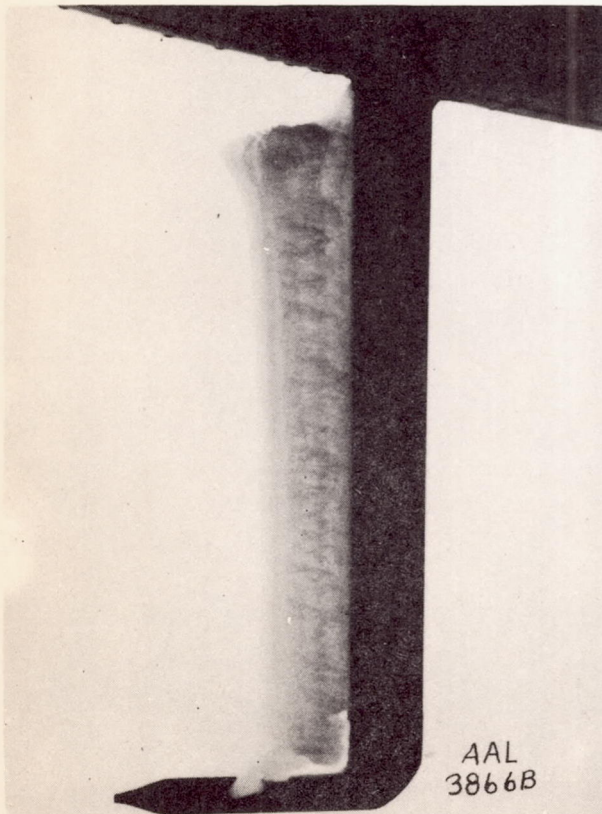


Figure 44.- Ice accumulation on the right airspeed mast during test 7. (Photograph taken after landing.)



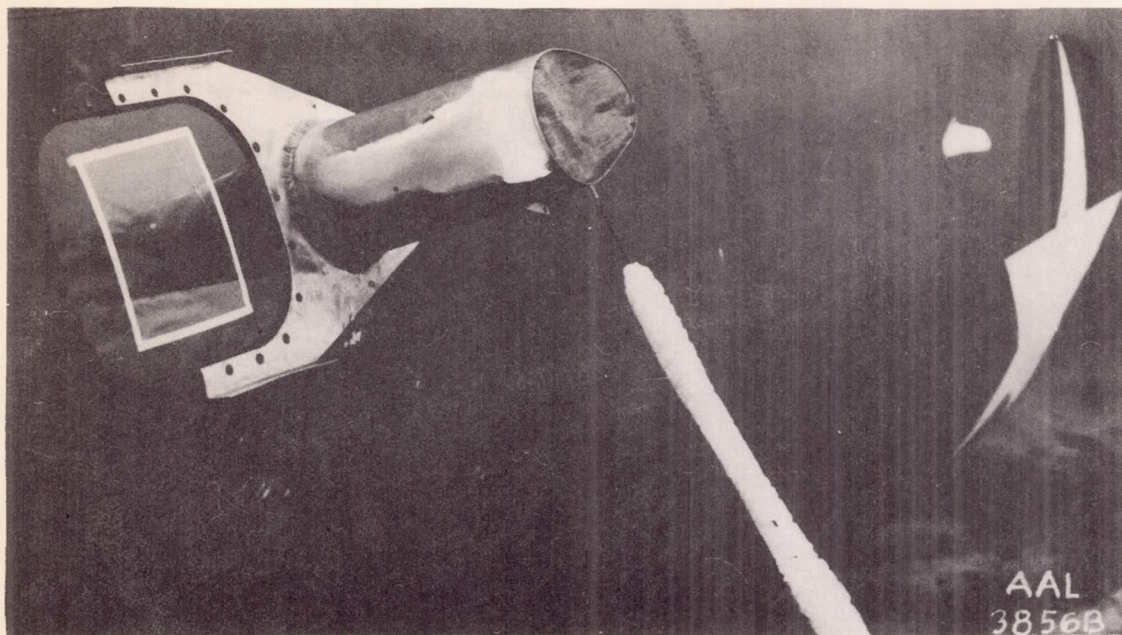


Figure 45.- Ice accumulations on the ice-indicating strut and on the lead-in antenna wire of the liaison radio. Photograph was taken after landing from test 7.

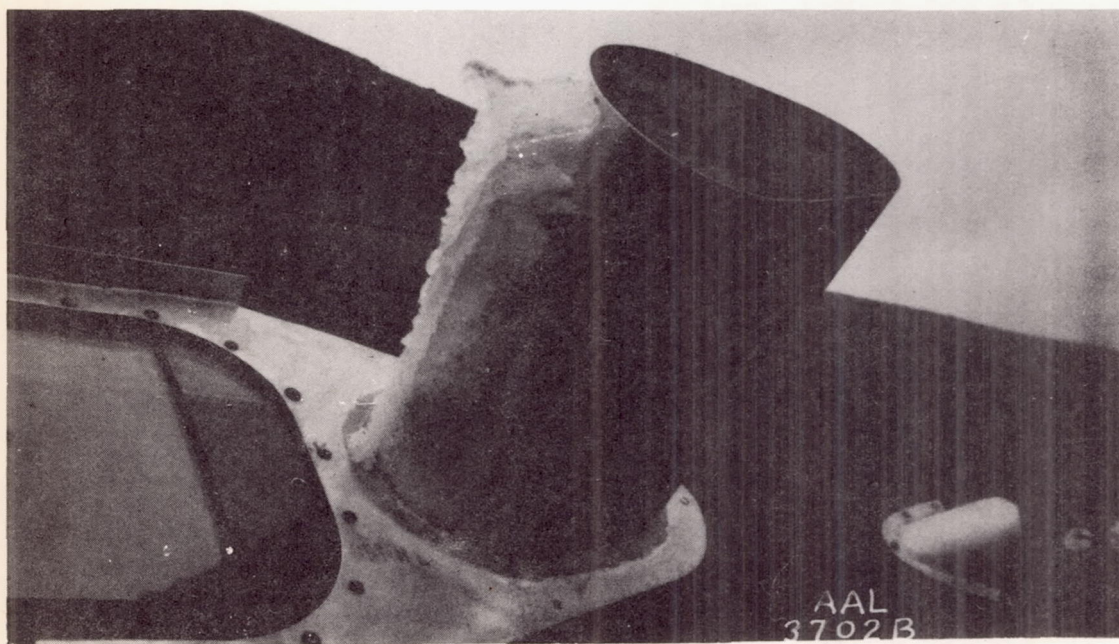


Figure 46.- Ice accumulation on the ice-indicating strut, mounted on the left side of the fuselage at the radio compartment during the flight on February 23, 1943. (Photograph taken after landing.)